USE OF QUANTUM MECHANICAL

CALCULATIONS TO INVESTIGATE SMALL

SILICON CARBIDE CLUSTERS

THESIS

Jean W. Henry

AFIT/GAP/ENP/01M-04

DEPARTMENT OF THE AIR FORCE
AIR UNIVERSITY
AIR FORCE INSTITUTE OF TECHNOLOGY

Wright-Patterson Air Force Base, Ohio

USE OF QUANTUM MECHANICAL

CALCULATIONS TO INVESTIGATE SMALL

SILICON CARBIDE CLUSTERS

THESIS

Jean W. Henry

AFIT/GAP/ENP/01M-04

DEPARTMENT OF THE AIR FORCE
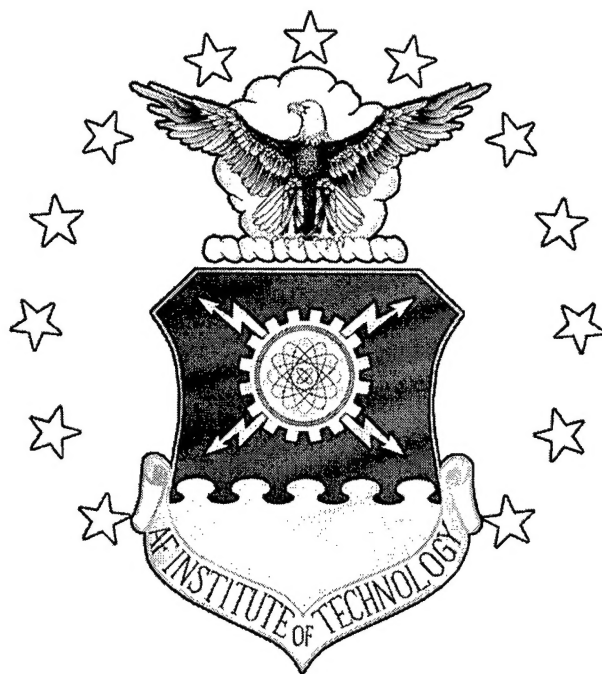**AIR UNIVERSITY**
AIR FORCE INSTITUTE OF TECHNOLOGY

Wright-Patterson Air Force Base, Ohio

USE OF QUANTUM MECHANICAL CALCULATIONS TO INVESTIGATE SMALL SILICON CARBIDE CLUSTERS

THESIS

Jean W. Henry

AFIT/GAP/ENP/01M-04

USE OF QUANTUM MECHANICAL CALCULATIONS TO

INVESTIGATE SMALL SILICON CARBIDE CLUSTERS

THESIS

Presented to the Faculty

Department of Physics Engineering

Graduate School of Engineering and Management

Air Force Institute of Technology

In Partial Fulfillment of the Requirements for the

Degree of Master of Science in Applied Physics

Jean W. Henry, B. S.
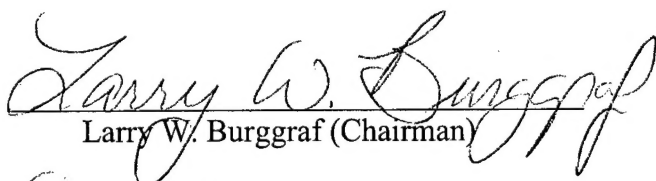
March 2001

AFIT/GAP/ENP/01M-04

USE OF QUANTUM MECHANICAL CALCULATIONS

TO INVESTIGATE SMALL SILICON CARBIDE CLUSTERS

Jean W. Henry
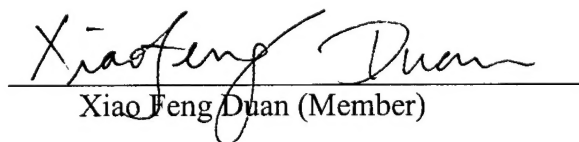
Approved:

_____   5 Mar 01
Larry W. Burggraf (Chairman)   date

_____   5 Mar 01
David E. Weeks (Member)   date

_____   5 Mar 01
Xiao Feng Duan (Member)   date

Acknowledgements

I would like to express my sincere appreciation to my faculty advisors, Dr. Larry W. Burggraf and Dr. David Weeks, for their extra teaching and guidance throughout the course and this thesis effort. Their teaching and supporting are greatly appreciated. I would also like to thank Dr. Frank X. Duan for his help and guidance in the computational portion of my thesis, and many useful discussions. I would like to thank the Dayton Area Graduate Studies Institute (DAGSI); I would never have this great opportunity to study at Air Force Institute of Technology (AFIT) without DAGSI scholarship. I would like to thank the entire faculty who has helped me at AFIT; I have learned a lot and enjoyed learning here. I would like to thank my husband and my daughter for their encouragement and support.

Jean W. Henry

Table of Contents

List of Figures

List of Tables

Abstract

Silicon carbide (SiC) has a wide band gap at high temperature, a good candidate material to meet future Air Force needs for wide-band-gap semiconductor devices for opto-electronics and high power electronics in aerospace applications. Defects generated during growth and fabrication are largely responsible for degradation of SiC properties, so surface chemistry of SiC is very important in the surface fabrication and control of epitaxial SiC films. Computer simulation is an economic and efficient approach to model the surface chemistry of silicon carbide. A hybrid quantum mechanics/molecular mechanics (QM/MM) method had been proven a sufficient way to model bulk SiC surfaces. In this method a small cluster modeled by a QM method is embedded in a bulk framework that can be modeled by a MM method. The key to use the QM/MM to model silicon carbide surface chemistry is to find a QM method that can accurately model the silicon carbide clusters.

Density Functional Theory (DFT) is chosen as a QM calculation method in this paper. Comparing the DFT calculation results with experimental results, the calculation results of geometry predictions, electron affinities (EA) and vibration frequencies are in good agreement with the experimental results. Sixteen optimized ground state structures were found using DFT:3BLYP method for the Si_mC_n ($m \leq 4, n \leq 4$) system. A root mean square average EA offset of -0.1 eV is found compared with the available experimental results. The factors that affect the accuracy of electron affinity calculation are discussed. The CPU time scaling of DFT calculations in SiC systems is also discussed.

USE OF QUANTUM MECHANICAL CALCULATIONS TO INVESTIGATE SMALL SILICON CARBIDE CLUSTERS

I.   Introduction

1.1 Motivation

Silicon carbide (SiC) has a wide band gap, high electron mobility, high breakdown field, high thermal conductivity, radiation resistance, and good mechanical properties at very high temperature [1], excellent chemical stability, high stiffness, and high hardness [2]. As a result, SiC has great promise in a wide variety of applications in both commercial and military sectors. These include uncooled electronics in space systems, high temperature electronics for turbine engine control, automotive applications, and well logging. Moreover, silicon carbide is a good candidate material to meet future Air Force needs for wide-band-gap semiconductor devices for opto-electronics and high power electronics in aerospace applications.

At present, the processing chemistry of silicon carbide is not well known. To know the surface chemistry of silicon carbide is very important for fabricating semiconductor surfaces and controlling epitaxial silicon carbide film growth. Particularly important are carbon-rich defects produced during etching and oxidation. Accurate computer simulations can provide the understanding of surface chemistry at atomic and molecular level for etching and oxidation. It will

1

be a significant step in controlling the performance of silicon carbide semiconductor devices if mechanism of defect formation is understood. Hence modeling the surface of silicon carbide bulk material is interesting. (Bulk defects are also of interest because bulk defects produced by SiC irradiation are important for space applications.)

The chemical reactions on surfaces are often modeled using molecular clusters. To accurately model small clusters, high-level ab initio quantum mechanical (QM) computational methods are needed. To understand the basic idea of molecular modeling, the basic concepts of quantum calculation methods are summarized.

1.2 Quantum Calculation Method Glimpse

Discussion of the principles used in quantum calculation methods can be found in the next chapter. Descriptions of the abbreviation of commonly used to describe semi-empirical methods, ab initio methods and density functional theory methods are listed in Appendix A. Briefly, quantum mechanical calculation methods are classified into three areas, which are described below:

1.2.1 Semi-empirical Methods (SE). SE methods use approximate methods to solve the matrix element integrals found in quantum chemistry methods for solving the Schrödinger equation. Some are taken from experiment data, some are neglected, and some are estimated by fitting to experimental data. SE should only be used for chemical species similar to those for which it is

parameterized. Since the experimental parameters used are generally not determined for compounds in unusual bonding situations, or distorted compounds, it may produce unreliable results for strained bonding. Based on the different approximation levels, SE methods have various implementations and commercial packages. The methods include completed neglect of differential overlap (CNDO); intermediate neglect of differential overlap (INDO); neglect of diatomic differential overlap (NDDO); modified neglect of differential overlap (MNDO); Austin Model 1 (AM1), an extension of the earlier MNDO/3 Hamiltonian. SE methods are often used to model large systems that cannot be practically modeled using ab initio methods. In this paper, we will use the AM1 method for comparison.

1.2.2. Ab initio Computations.

Ab initio methods are first principle methods that do not require empirical parameters and can be used for any molecular system. They usually use the Hartree-Fock (HF) method as a starting point to solve the Schrödinger equation using the self-consistent-field (SCF) iteration process.

The HF method uses the Hartree average potential to approximately treat a many electron system as a single electron in the average field that generated by the other electrons and nucleus. This makes it possible for one to solve a multi-electron Schrödinger equation. The wave function represents the molecular orbital, which is a linear combination of atomic orbitals (LCAO). Each of the atomic orbital is represented by a single electron wave function that is formed

3

from a number of functions called basis set functions.

The famous Variational Principle applies to all ab initio methods. It states that for an approximate wave function the approximate energy is always greater than the exact energy. So the lower the energy, the more accurate is the calculation. In Hartree-Fock approximations, the average potential assumption ignores the electron-electron correlation, thus HF has its limits in modeling energy and cannot accurately model electronic correlation energy in electron rich systems. For higher level ab initio calculation methods (post HF), such as multi-configuration self-consistent-field (MCSCF), or complete active space (CAS). MCSCF and CAS calculation methods consider electron correlation. They are proven accurate calculation methods, which are exhaustively used by physicists and chemists. But they are computationally expensive.

The wave function is represented as a linear combination of N-electron trial functions. In post HF calculations, if the basis were complete, one would obtain the exact energies not only of the ground state but also of all excited states of the system. However, in reality only a finite set of N-electron trial functions is used. Increasing the size of basis set results in the more accurate energy. On the other hand, increasing the basis set will dramatically increase the computing time. Unlike SE methods, ab initio methods require computing each of the matrix element integrals in solving Schrödinger equation, therefore, they are very time consuming and may not be practical for large systems.

1.2.3. Density Functional Theory (DFT) Methods.

DFT methods combine the theory of statistical physics with quantum chemistry. Kinetic energy and potential energy are represented as functions of electron density for a stationary state. DFT methods can simplify the problem of solving wave function to an easier problem of solving the electron density, $\rho = \Psi^* \Psi$. The Hamiltonian is a functional of electron density. In Density Functional Theory, the functional terms and the corresponding coefficients are optimized using statistics physics and experimental results, so the average electron correlation is considered. This leads to more accurate result than a HF method. In this work, DFT:B3LYP method [3] is used, which uses a hybrid functional with parameters from statistical physics and HF molecular orbital theory. A brief comparison of the three methods is listed in the Table 1.

Table 1. A brief comparison of different calculation method

Calculation Method	Semi-empirical (SE)	DFT	Ab initio
Accuracy	Not reliable	Good	Good
Cost	Cheap	Expensive	Very expensive
Larger System (>20 atoms)	Very fast	Unknown	Impractical
Ground State	OK	Good	Good
Excited State	OK	Restricted	Very good
Electron affinity Calculation	Good	Excellent	OK
Geometry Optimization	Poor	Good	Very good

Table 1 shows that SE methods have the advantage of being fast, ab initio methods have the advantage of being accurate, but impractical for large systems, and DFT has advantage of being accurate and efficient, but its usage is limited to

the ground electronic state.

1.3 Previous Research Review

Surfaces are often modeled using molecular clusters, which are too small to accurately represent the mechanical environment of bulk materials. Even these small sized clusters require high cost in computation time using ab initio methods with large basis sets. In order to accurately model chemical reactions at a surface, the clusters are required to be large enough to represent the bulk material. For such a large system, an accurate calculation of very large clusters using large basis sets by ab initio method is impractical. Shoemaker [4] has successfully modeled Si and SiC surface chemistry using a hybrid Quantum Mechanics and Molecular Mechanics (QM/MM) method. He used the quantum ab initio calculations to optimize a small cluster embedded in a large system, which can be calculated by Molecular Mechanics (MM) method. This new embedded cluster model is called the Surface Integrated Molecular Orbital / Molecular Mechanics (SIMOMM). In this method, the 'action' region where the actual chemical occurs is treated quantum mechanically, while the spectator region that primarily provides the effect of the surrounding bulk is treated using molecular mechanics. It has been shown that SIMOMM is especially effective for a system, such as semiconductors, in which the surface reaction is localized [16]. The key of the SIMOMM model is to combine a highly accurate ab initio method with a highly efficient molecular mechanics method. This approach minimizes time-consuming electronic structure computations while maintaining the effect of the

6

"bulk" constraint. It is less useful for conductors with large electronic delocalization.

In order to find the optimized cluster structure, many studies have been done on pure carbon or pure silicon [17-20]. Carbon-carbon bonds have significant σ and π bonding, which favors linear minimum energy structures for carbon cluster structures. Silicon-silicon mostly involves σ bonding. The minimum energy structures of silicon clusters tend to have three-dimensional structure. Study of molecular sized silicon carbide clusters compared to carbon clusters and silicon clusters is of fundamental interest. Recent studies on SiC clusters are summarized in Table 2.

Shown in Table 2, Rittby [5,6,7] reported geometry optimization studies on Si_2C, Si_3C, and C_2Si_3 clusters, using a Hartree-Fock method with a low-level basis set: 6-31G. The ground state structures of these clusters were found to be linear. This compares well with the previous experimental result that reported by Karfafi [9-11] using IR spectroscopy. V.D. Gordon [12] calculated SiC_4 and SiC_6 cluster, using low level to very high level ab initio method, with medium size and large size basis sets. Compared to the experiments by McCarthy [13] using Fourier transform microwave spectroscopy (FTM), the calculation is in good agreement with experiment. Duan et al. [14] from our group intensively studied the Si_2C_3 cluster using various calculation methods. Comparing the electron affinity calculated by a DFT method with the experiment result by Dr. Lineberger's [15], the average absolute error is only -0.027 eV, which is excellent agreement with the experimental result. Electron affinity was found to be more

sensitive to the accuracy of the calculation than structure or vibration frequencies.

Table 2. A summary of previous research on Si_mC_n clusters

Cluster	Experiment Method & Research Group	Calculation Method*	Research Group	Calculation Accuracy vs. Experiment
Si_2C, Si_3C, Si_2C_3	IR Spectrum By Z. H. Kafafi [8] W.R.M. Graham [9-11]	HF/6-31G	C. M. L. Rittby [5,6,7]	3% average error to frequencies, intensities and isotopic shifts 4% error to isotopic shifts
SiC_4 SiC_6	Fourier transform microwave (FTM) Spectroscopy By M.C. McCarthy [13]	DFT-B3LYP/ cc-pV5Z /cc-pVDZ CCSD (T) CCSD-T CCSD MP2, HF-SCF	V. D. Gordon [12]	Average error of bond length is less than 0.0015Å
Si_2C_3	Photoelectron spectroscopy (PES) By Lineberger et al [15]	HF/ cc-pVDZ MP2/ cc-pVDZ//HF/ cc-pVDZ DFT-B3LYP/cc-pVDZ DFT-B3LYP/cc-pVTZ+ // B3LYP/ cc-pVDZ DFT-B3LYP/cc-pV5Z+ // B3LYP/ cc-pVDZ MCSCF(20,20)/cc-pVDZ CAS(8, 10)/cc-pVDZ+ MCQDPT2(8, 10)/cc-pVDZ+// CAS(8, 10)/cc-pVDZ+	X. Duan [14]	Using DFT:B3LYP/ aug-cc-pV5Z // B3LYP/ cc-pVDZ 0.027 eV absolute EA error Using MP2/ cc-pVDZ//HF/ cc-pVDZ 0.435 eV absolute EA error Using DFT:B3LYP/ cc-pVDZ 0.257 eV absolute EA error

* For detailed descriptions of calculation method and basis set please see Appendix A

1.4 Problem Statement

In order to model silicon carbide surfaces using the QM/MM method, the key is to find the QM methods that can accurately predict the structure and electronic properties of silicon carbide clusters. It is also fundamentally interesting to compare silicon carbide cluster molecules with pure silicon and pure carbon clusters. It has been learned from previous research by Duan et al that DFT provides more accurate electron affinity results and takes less computer time than ab initio MP2 and CAS calculations using the same basis sets [14]. Based on these results, DFT: B3LYP is selected as the main QM method in this work.

1.4.1. Comparison with Experimental Results.

After choosing the QM method, it is used to find optimized minimum energy or stable structure of each silicon carbide cluster (Si_mC_n). To make sure of the accuracy of the calculation, comparison of calculation results is made with experimental results for observed clusters. We collaborate with Dr. Lineberger's group, who conduct PES experiments on silicon carbide clusters produced by a cathode discharge. Their results are listed in Table 3 for Si_mC_n (m+n=4, 5, 6, 7, 8) clusters mass selected from the plume. These gas phases Si_mC_n clusters have analogy with surface or bulk defects of silicon carbide that we wish to be able to model.

Table 3. Experimental results using Photo Electron Spectroscopy (PES) on Si_mC_n clusters by Dr. Lineberger's group at the University of Colorado

m+n	4		5		6	7	8
Cluster	C_3Si	CSi_3	C_4Si	C_3Si_2	C_4Si_2	C_5Si_2	C_6Si_2
Electron Affinity EA (eV)	2.845 (2.839)	1.535	2.327	1.769	2.556	2.136 (2.131)	2.049
Frequency cm^{-1}	-48	315	565	420	845	40	3735
	1950	490	1105	910	1175	340	
	2015	12575	2120	1485	1860	8105	
	2185		2720	1930	2665		
				3905			
Geometry Information	Anion: linear Neutral: rhombic. C_{2v}, Linear nearly degenerate, $C_{\infty v}$	Anion: rhomboidal $C_{\infty v}$ Neutral: Rhomboidal	Anion: Linear Neutral: Linear	Anion: Linear $C_{\infty h}$ Neutral: Linear	Anion: Linear $C_{\infty h}$ Neutral: Linear	Anion: Linear Neutral: Linear	

1.4.2. Factors Influencing Molecular Modeling. The size of the

molecular model of the Si_mC_n cluster is also important. As the numbers m and n

increase, the cluster structure predicted from molecular modeling will approach

the structures that can represent the bulk material well. However, in this paper,

we will only accomplish the molecular modeling for small size gas phase Si_mC_n

clusters due to limited time.

Choice of basis set for the composite of trial wave function may greatly

affect the calculation result. A larger basis sets gives more potential for accurate

description of the wave function. Therefore, the effects of basis set used during

calculations will be investigated. From the practical viewpoint, the time scaling

of the DFT method with cluster size and the size of basis sets is worth some effort

too. So far, no one knows the time scaling of DFT calculation for SiC systems.

Semi-empirical methods are fast and are used to model large systems. But SE methods are only good for those systems that the parameters suit (please see early section 1.1). A semi-empirical method, AM1, which is parameterized for silicon compounds, will be studied for silicon carbide systems. Comparisons with experimental result will reveal the accuracy and reliability of AM1 calculations.

1.5 Objective Scope

The objective is to apply DFT: B3LYP as the QM calculation method, AM1 as the semi-empirical method to model silicon carbide clusters. Restricted open shell method, ROHF, is used in AM1 calculations, the restricted open shell method, RODFT, is used in DFT calculations.

1) Si_2C_3 isomer geometry predictions using AM1 method will be compared with ab initio methods [14] and with the experimental results [15]. Predictions of geometry, electron affinity and vibration frequency calculations will also be perform on Si_mC_n clusters (m + n = 4, 5, 6, 7, 8) using the AM1 method for comparison with experiment results [15] to reveal the accuracy of AM1 calculation for the Si_mC_n system.

2) To find the quantum mechanical method that can accurately model SiC is the goal. In this work, the density functional theory DFT: 3LYP method is selected. First, we compute ground state structures of SiC clusters using the DFT method. The structures will be mapped out as shown in Table 4.

Table 4. The mapping table of DFT calculation on Si_mC_n cluster

C_n \ Si_m	1	2	3	4
1	T_0	S_0	S_0	S_0
2	S_0	S_0	S_0	S_0
3	T_0	S_0	S_0	S_0
4	S_0	T_0	S_0	S_0

T_0 indicates a triplet state; S_0 indicates a singlet state.

As the number of Si atoms (m) and carbon atoms (n) increase, the model discussed in this paper will be increasingly closer to bulk SiC materials. This work will focus on the range $m \leq 4, n \leq 4$.

3) Based on the structure, the electron affinity and vibration frequencies of each cluster will be calculated by the DFT method. The accuracy and the reliability of DFT calculations will be investigated by comparing the calculation results with available experimental results [15]. After the comparison, we will know if the DFT method can accurately describe SiC systems. Then other factors that may affect the accuracy of calculation will be investigated, such as the size of basis size, the properties of basis sets (adding diffuse functions in basis sets). The CPU time scaling of DFT

calculations will be discussed from two directions, one is the time scaling with the size of basis sets, and the other is the size of the cluster.

1.6 Thesis Outline

<u>Chapter one</u>:   The first chapter will introduce QM modeling methods, describe the importance of silicon carbide material and the purpose of modeling SiC surface chemistry, and outline the research plan.

<u>Chapter two</u>:   The second chapter introduces quantum chemistry theory and the calculation principles that are used in this paper. It classified into following steps:

1) Basic concepts and principles of quantum chemistry.

2) The fundamental principle of ab initio calculation: Hartree-Fock self-consistent-field (HF-SCF).

3) Semi-empirical method AM1 based on the HF-SCF.

4) The Density Functional Theory (DFT).

<u>Chapter three</u>:   The third chapter compares the AM1 method calculation results with DFT calculation results and with experimental results. It points out where AM1 method fails to accurately model the SiC system.

<u>Chapter four</u>:   The fourth chapter compares DFT calculation results with experimental results pointing out that the DFT method successfully models the ground state SiC system. The factors that affect the accuracy of DFT calculation,

such as the basis set, the property of basis sets are investigated. The relationship

of the DFT computation time with the size of system is also discussed.

Chapter five: Summary and conclusions are given in the last chapter.

II. An Overview of Quantum Computational Theory

In this chapter, sections 2.1-2.5 follow the theory of *Attila Szabo* and *Neil S. Ostlund* in "Modern Quantum Chemistry", with detailed discussion and examples [21]

2.1 One Particle Wave Equation

Since Austrian physicist Erwin Schrödinger found a differential equation in 1925, the so-called wave equation, the soul of quantum theory has been how to solve this partial differential equation (PDE) $\hat{H}\Psi = E\Psi$ (where $\hat{H}$ is the Hamiltonian operator, Ψ is the wave function and E is total energy). The wave function contains all the information in which physicists and chemists are interested. In most cases, one is concerned with atoms and molecules without time-dependent interactions, the time-independent Schrödinger equation. For a single particle system, such as hydrogen atom, the coulomb potential is only related to the distance between electron with nucleus, ie., the Hamiltonian only have one variable, r, so one can use separable variables method; then it is not difficult to solve the PDE, the solutions of which have the form:

$$\Psi(r,\theta,\phi) = \psi(r)\Theta(\theta)\Phi(\phi) \tag{2-1}$$

2.2 Many Electron Wave Function

For N, number of electrons, and M, number of nuclei, using A and B to represent the nuclei, and i, j to represent the electrons, if R_A, R_B represent the position of nuclei and r_i, r_j represent the position of electrons in Cartesian

15

coordinates, the Hamiltonian can be written as:

$$\hat{H}_{Total} = \sum_{i=1}^{N} \frac{1}{2}\nabla_i^2 \qquad \text{Electronic kinetic energy}$$

$$+\sum_{i=1}^{M} \frac{1}{2M_A}\nabla_A^2 \qquad \text{Nuclear kinetic energy}$$

$$-\sum_{i=1}^{N}\sum_{A=1}^{M} \frac{Z_A}{r_{iA}} \qquad \text{Electron-nucleus coulomb potential (attractive)}$$

$$+\sum_{i=1}^{N}\sum_{j>i}^{M} \frac{1}{r_{ij}} \qquad \text{Electron-electron coulomb potential (repulsive)}$$

$$+\sum_{A=1}^{M}\sum_{B>A}^{M} \frac{Z_A Z_B}{R_{AB}} \qquad \text{Nucleus-nucleus coulomb potential (repulsive)}$$

(2-2)

Then the Schrödinger equation will look like:

$$\hat{H}_{Total}\Psi(r1,r2,r3,....rN) = E\Psi(r1,r2,r3,.....rN) \quad . \qquad (2\text{-}3)$$

The solution to this PDE is a wave function in which nuclear and electronic

motions are coupled and the electron-electron motions are coupled. Because of

the coupling term in the Hamiltonian expression, one cannot apply the variables

separable principle to solve the PDE. We cannot solve this problem exactly, so

certain approximations are necessary.

2.2.1. Born-Oppenheimer Approximation. American physicists Born and

Oppenheimer suggested that one could approximately treat the nuclear positions

as fixed at R_A (R_A is a parameter, related to chemical bond lengths), because the

great difference in mass of electrons and nuclei. Electrons move very fast around

nuclei; nuclei move very slowly by comparison to electrons. Thus, the electronic

wave function depends explicitly on the electron coordinates and parametrically

on the nuclear coordinates under the Born-Oppenheimer approximation. The R_A

parameterized electronic Hamiltonian can be written as:

$$H_{el} = \sum_{i=1}^{N} \frac{1}{2} \nabla_i^2 \qquad \text{Electronic kinetic energy}$$

$$-\sum_{i=1}^{N} \sum_{A=1}^{M} \frac{Z_A}{\left(\vec{r}_i - \vec{R}_A\right)} \qquad \text{Electronic coulomb potential at fixed nuclear}$$

coordinate $\vec{R}_A$

$$+\sum_{i=1}^{N} \sum_{j>i}^{M} \frac{1}{r_{ij}} \qquad \text{Electron-electron coulomb potential}$$

H_{el}, the electronic Hamiltonian, can be further simplified as:

$$H_{el} = \sum_{i=1}^{N} (\frac{1}{2} \nabla_i^2 - V_i(r_i)) + \sum_{i=1}^{N} \sum_{j>i}^{N} \frac{1}{r_{ij}} \qquad (2\text{-}4)$$

$$= \sum_{i=1}^{N} h_i + \sum_{i=1}^{N} \sum_{j>i}^{N} \frac{1}{r_{ij}} \qquad (2\text{-}5)$$

where $\sum_{i=1}^{N} h_i$, called core Hamiltonian, denoted as H_{el}^{core}, is independent from the

electron-electron coupling $\sum_{i=1}^{N} \sum_{j>i}^{N} \frac{1}{r_{ij}}$. The electron-electron coupling potential,

makes the PDE too difficult to solve directly. Perturbation theory is used to

obtain approximate solution. Approximate solutions can be improved and

enhanced based on the Variational Principle.

2.2.2. Variational Principle.

The time-independent Schrödinger equation is an eigenvalue equation:

$$\hat{H}_{Total}|\psi\rangle = E|\psi\rangle \qquad (2\text{-}6)$$

Where $\hat{H}_{Total}$ is a Hermitian operator, $|\psi\rangle$ is the wave function represented as a linear combination of basis sets, and E is the energy. For a many particle system, the Schrödinger equation cannot be solved exactly, one need to find an approximate approach to the solutions of the eigenvalue equations. One can select the solutions to be normalized wave functions:

$$\langle\psi|\psi\rangle = 1 \qquad (2\text{-}7)$$

To solve this PDE, the wave function is required to be well behaved and satisfy appropriate boundary conditions (e.g. vanish at infinity). The expectation value of the Hamiltonian, is an upper bound to the exact ground state energy.

$$\langle\psi|\hat{H}|\psi\rangle = E|\psi\rangle \qquad (2\text{-}8)$$

Using Lagrange's indeterminate multipliers method, mathematical manipulation can easily prove that:

$$\langle\psi|\hat{H}|\psi\rangle \geq E_0|\psi\rangle \qquad (2\text{-}9)$$

The equality only holds when:

$$|\psi\rangle = |\psi_0\rangle \qquad (2\text{-}10)$$

Since $E \geq E_0$, one's interest is to find the minimum energy of this eigenfunction. The lower the energy one finds, the higher the accuracy.

2.3 Electronic Wave Function

2.3.1. The Anti-symmetry Principle.

Electrons are identical, moving rapidly around the nuclei with either spin up or spin down. Because the non-relativistic Hamiltonian operator makes no reference to spin, we simply make the wave function dependent on spin. Without concerning spin, a two electron system with one electron at position (x_1, y_1, z_1) and the another at (x_2, y_2, z_2), the general wave function is $\Psi(x_1, y_1, z_1, x_2, y_2, z_2)$. For simplicity of notation $\Psi(x_1, y_1, z_1, x_2, y_2, z_2)$ is abbreviated as just $\Psi(\bar{1}, \bar{2})$, with $\bar{1}$ representing the coordinates of particle 1 and $\bar{2}$ representing the coordinates of particle 2. The probability of finding the first particle within the differential volume $d\tau_1 = dx_1 dy_1 dz_1$ and the second particle within $d\tau_2 = dx_2 dy_2 dz_2$, integrated over all space, the total probability of all possible arrangements of the two particles must be unity, giving the normalization condition:

$$\iint \Psi^*(\bar{1}, \bar{2}) \Psi(\bar{1}, \bar{2}) d\tau_1 d\tau_2 = 1 \tag{2-11}$$

The probability distribution $\Psi^2 = \Psi^* \Psi$ should be unaffected by changes in the arbitrary particle labels,

$$\Psi^2(\bar{1}, \bar{2}) = \Psi^2(\bar{2}, \bar{1})$$

$$\Psi(\bar{1}, \bar{2}) = \pm \Psi(\bar{2}, \bar{1})$$

Bosons particles have integral spin; Fermions particles have half spin. Thus, all wave functions must be either symmetric (+) or anti-symmetric (-) with regard to exchange of the labels of any identical particles, under the condition of ignoring

the spin effect. With the spin, therefore, an additional requirement must added to a wave function: a many-electron wave function must be anti-symmetric with respect to the interchange of the coordinates x both space and spin for any two electrons, this also called the anti-symmetry principle. It can be denoted as:

$$\Psi(x_1,\cdots,x_i,\cdots,x_j,\cdots,x_N) = -\Psi(x_1,\cdots,x_j,\cdots,x_i,\cdots,x_N) \qquad (2\text{-}12)$$

2.3.2. Spin Orbitals and Spatial Orbitals.

An orbital is defined as a wave function for a single particle (e.g. an electron). A molecular orbital is the molecular electronic wave function. The spatial portion of a molecular orbital, a spatial orbital, $\psi_i(r)$ is a function of the particle's position vector $\mathbf{r}$. A spin orbital is the spatial orbital with a factor designing spin up (denoted by α) or spin down (denoted by β). So, $|\psi_i(r)|^2 dr$ is the probability of finding the electron in the small volume element dr at the distance $\mathbf{r}$ (where $\mathbf{r}$ is a position vector).

Spatial molecular orbitals form an orthonormal set such that:

$$\int \psi_i^*(r)\psi_j(r)dr = \delta_{ij} \qquad (2\text{--}13)$$

If the set of spatial orbitals $\{\psi_i\}$ were complete, then any arbitrary function could be written as $f(r) = \sum_i^\infty C_i\psi_i(r)$, where the C_i are constant coefficients. The spin orbital can be denoted by spatial orbital with spin factor:

$$\chi_{(r)} = \begin{cases} \psi_\alpha(r) \\ \psi_\beta(r) \end{cases} \qquad (2\text{--}14)$$

where α represents spin up, β represents spin down. If spatial orbitals are orthogonal, the spin orbitals are orthogonal too.

$$\int \chi_i^*(x)\chi_j(x)dx = < \chi_i|\chi_j > = \delta_{ij} \tag{2-15}$$

2.3.3 Hartree Products.
Before considering the form of the exact wave function for a fully interacting system, neglecting electron-electron repulsion then equation (2–5) becomes:

$$\aleph = \sum_{i=1}^{N} h_i \tag{2-16}$$

Alternatively, $h_{(i)}$ might be an effective one-electron Hamiltonian that includes the effects of electron-electron repulsion in some average way. Thus, $h_{(i)}$ will have a set of eigenfunctions, which are a set of spin orbitals $\{\chi_j\}$.

$$h_{(i)}\chi_j(x_i) = \varepsilon_j\chi_j(x_i) \tag{2-17}$$

Because $\sum_{i=1}^{N} h_i$ is a sum of one-electron model Hamiltonians, a wave function which is a simple product of spin orbital wave functions for each electron, written as:

$$\Psi^{HP}(x_1, x_2, \cdots, x_N) = \chi_i(x_1)\chi_j(x_2)\cdots\chi_k(x_N) \tag{2-18}$$

is an eigenfunction of $\aleph$:

$$\aleph\Psi^{HP} = E\Psi^{HP}$$

The total energy E is just the sum of the spin orbital energies of each of the spin orbitals appearing in Ψ^{HP}:

$$E = \varepsilon_i + \varepsilon_j + \cdots + \varepsilon_k \tag{2-19}$$

Such a many-electron wave function, Ψ^{HP}, is called a Hartree product.

2.3.4 Slater Determinant.
A Hartree product is an uncorrelated electron wave function, because the probability of finding electron number one at a given point in space is independent of the position of electron number two when Ψ^{HP} is used. In reality, electron one and electron two are correlated; because of electron-electron repulsion electron one will "avoid" regions of space that occupied by electron two. Also, the Hartree product does not account of the indistinguishability of electrons, but specifies the electron one as occupying spin orbital χ_i, and the electron two as occupying χ_j. The antisymmetry principle requires electronic wave functions be antisymmetric with respect to the interchange of the space and spin coordinates of any two electrons. Therefore, Slater determinant is a better approach to write the electronic wave function as follows:

$$\Psi_{(r1,r2,...rN)} = \frac{1}{\sqrt{N!}} \begin{vmatrix} \chi_{1(r1)} & \chi_{2(r1)} & \cdots & \chi_{N1(r1)} \\ \chi_{1(r2)} & \chi_{2(r2)} & \cdots & \chi_{N(r2)} \\ \vdots & \vdots & \vdots & \vdots \\ \chi_{1(rN)} & \chi_{2(rN)} & \cdots & \chi_{1(rN)} \end{vmatrix} \tag{2-20}$$

where $\dfrac{1}{\sqrt{N!}}$ is a normalization constant and $\chi_{(r)}$ is a spin orbital. The Slater determinant wave function is commonly abbreviated as $\text{Det} \left| \Psi_{(r1,r2,\cdots,rN)} \right\rangle$.

22

Exchange of electrons corresponds to swapping two rows in the matrix, which will change the sign of the determinant satisfying the anti-symmetry requirement. If two columns in the matrix are identical, i.e. two electrons of the same spin are placed in the same orbital, the determinant is zero, as required by the Pauli exclusion principle.

2.3.5. Basis Sets. The choice of the trial wave functions is important to the solution. The most commonly used choice is linear combinations of atomic orbitals (LCAO). Since the atomic orbitals can be chosen as orthonormal functions, this is a finite generalized Fourier series expansion of the molecular orbitals. The atomic orbitals are composed of basis functions called a basis set. The basis sets are a summation of series expansion of electron spatial orbitals. The most common and the easiest approach is to use Slater function orbitals. Slater orbitals work well in describing the electron's properties, but unfortunately, they produce difficulties during computation. In order to increase calculation efficiency, some approximation and standard basis set functions are needed. If Gaussian functions are used instead of Slater functions the four-center integrals that are most time consuming in computation can be changed to two-center integrals. Two-electron integrals can be calculated rapidly and efficiently with Gaussian functions. However, Gaussian functions are not optimum basis functions and have functional behavior different from the known functional behavior of molecular orbitals.

The Minimal STO-3G Basis Set. One can use fixed linear combinations of the primitive Gaussian functions to form a contracted Gaussian:

$$\Phi_u^{CGF}(\mathbf{r} - \mathbf{R_A}) = \sum_{p=1}^{L} d_{pu}\Phi_u^{GF}(\alpha_{pu}, \mathbf{r} - \mathbf{R_A}) \tag{2-21}$$

Where L is the length of the contraction, d_{pu} is the contraction coefficient, α_{pu} is contraction exponent. By a proper choice of L, d_{pu}, and α_{pu}, the contracted Gaussian function can be made to assume any functional form consistent with the primitive functions used. For example, in the Figure 1, there is a least square fit a Slater 1s function. For L=1:

$$\Phi_{1S}^{CGF}(\xi = 1.0, STO-1G) = \Phi_{1S}^{GF}(0.270950) \tag{2-22}$$

For L=2:

$$\Phi_{1S}^{CGF}(\xi = 1.0, STO-2G) = 0.678914\Phi_{1S}^{GF}(0.151623) + 0.430129\Phi_{1S}^{GF}(0.851819) \tag{2-23}$$

For L=3:

$$\Phi_{1S}^{CGF}(\xi = 1.0, STO-3G) = 0.444635\Phi_{1S}^{GF}(0.109818)$$
$$+ 0.535328\Phi_{1S}^{GF}(0.405771) + 0.154329\Phi_{1S}^{GF}(2.22766) \tag{2-24}$$

Higher Level Basis Sets. The reason why we need higher basis sets is the Minimal STO-3G Basis Set (MGS) provides poor results, because MGS does not have the ability to expand or contract the orbital in response to different bonding situations. Theoretically, increasing the basis sets size will increasing the accuracy. On the other hand, higher level basis sets formed by adding specific

functions to the basis set, such as using a split-valence or 'double zeta' technique to treat the electrons in different sub-shells differently, as well as the polarization and the size of atoms, can also improve the quality of basis set. Commonly used basis sets are listed in Appendix A.
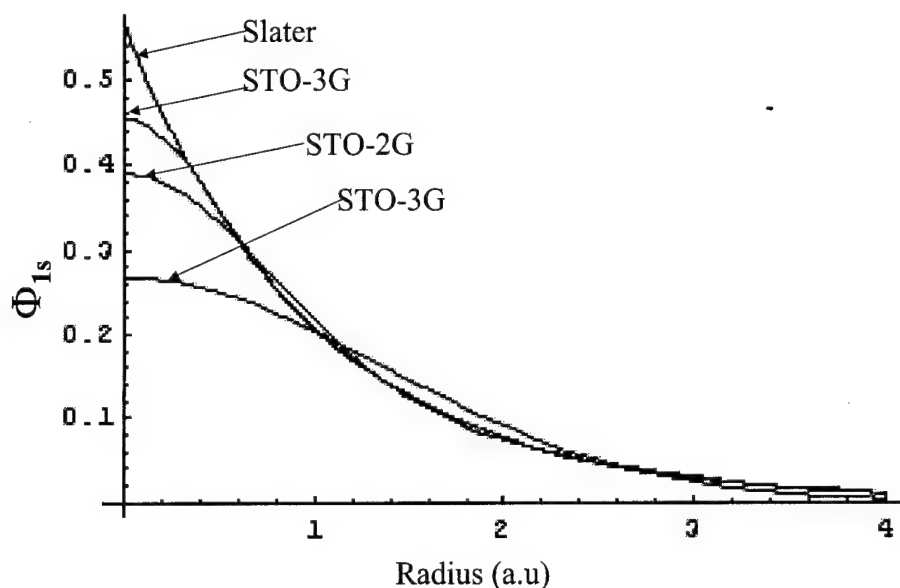
Figure 1. The quality of the least-squares fit of a 1s Slater function obtained at the STO-1G, STO-2G, and STO-3G ($\zeta = 1$)

Larger sized basis sets result in more accurate results. Using infinite of basis set we may get the exact solution. However, the actual calculation methods have their limits because the currently used methods are all finite approximate methods. The dependence of calculations on size of one-electron and N-electron basis sets is summarized in Figure 2. When one adds up all those terms in the molecular orbitals, the Hartree-Fock calculations become complex very quickly.

For example, consider the diatomic molecule HF, for six atomic orbitals to represent each molecular orbital. If one uses 6 Gaussian functions to represent each atomic orbital, one would have $36 \times 36 \times 6$ complicated integrations to perform for a single iteration of the HF- SCF calculation procedure. Sometimes, we have to trade off accuracy with cost.
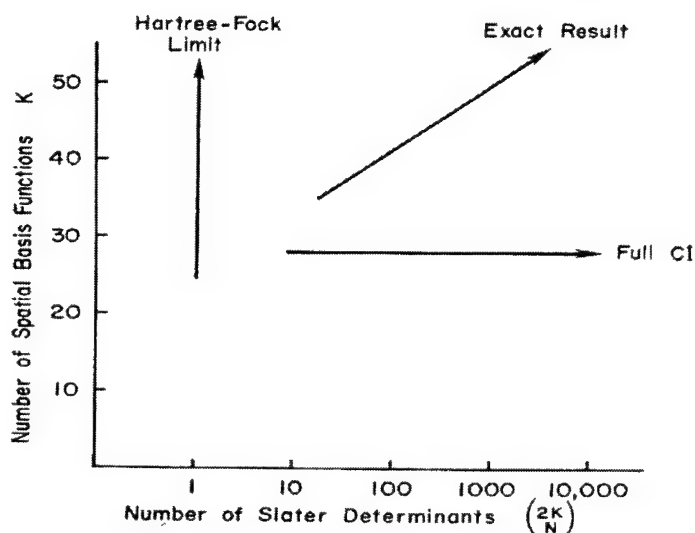
Figure 2. Dependence of calculations on size of basis sets

2.4 Ab Initio Hartree-Fock Self Consistent Field (HF-SCF)

<u>**2.4.1. Hartree-Fock Approximation.**</u> Assume there is an average static electric field generated by (N-1) electrons to form a spherical potential $V_i(r)$ which is centered at the nucleus. $V^{HF}(i)$ are called Hartree-Fock potentials. With this assumption, a many particle system can be broken down to a single electron system, under the condition of an average potential $V^{HF}(i)$. Define the Fock operator as:

$$f(i) = \sum_{i=1}^{N} (\frac{1}{2}\nabla_i^2 - V_i(r_i)) + V^{HF}(i) \qquad (2\text{--}25)$$

where $f(i)$ is an effective one-electron operator. Under this one-electron model, Schrödinger equation can be written as:

$$f(i)\chi(x_i) = \varepsilon\chi(x_i) \qquad (2\text{--}26)$$

The solution of PDE equation (2–26) yields a set of orthonormal Hartree-Fock spin orbitals $\{\chi_k\}$ with orbital energies $\{\varepsilon_k\}$. Now one attempts to find a set of spin orbitals $\{\chi_a\}$ to form a Slater determinant wave function

$$|\Psi_0\rangle = |\chi_1\chi_2\cdots\chi_a\chi_b\cdots\chi_N\rangle \qquad (2\text{--}27)$$

According to the variational principle, the best spin orbitals are those which minimizes the electronic energy:

$$\begin{aligned}
E_0 = \langle\Psi_0|H \ |\Psi_0\rangle &= \sum_a \langle a|h|a\rangle + \frac{1}{2}\sum_{ab} \langle ab\|ab\rangle \\
&= \sum_a \langle a|h|a\rangle + \frac{1}{2}\sum_{ab}[aa|bb] - [ab|ba]
\end{aligned} \qquad (2\text{--}28)$$

One can systematically vary the spin orbitals $\{\chi_a\}$, constraining them to remain orthonormal:

$$\langle\chi_a|\chi_b\rangle = \delta_{ab} \quad , \qquad (2\text{--}29)$$

until the energy E_o is a minimum. In doing so, one obtains an equation that minimizes E_o. This equation is the Hartree-Fock integro-differential equation:

$$h(1)\chi_a(1) + \sum_{b\neq a}[\int |\chi_b(2)|^2 r_{12}^{-1}]\chi_a(1)dx_2 - \sum_{b\neq a}[\int \chi_b^*(2)\chi_a(2)r_{12}^{-1}dx_2]\chi_b(1) = \varepsilon_a\chi_a(1)$$

$$(2\text{--}30)$$

Where h(1) is the core Hamiltonian, χ_a is the best spin orbital that minimizes the

energy, χ_b is the other possible spin orbital. To simplify the equation (2–30),

define the coulomb operator:

$$J_b(1) = \int |\chi_b(2)|^2 r_{12}^{-1} dx_2 = \int \chi_b^*(2) r_{12}^{-1} \chi_b(2) dx_2 \qquad (2\text{–}31)$$

Where $J_b(1)\chi_a(1)$ represent electron one in χ_a experiencing a one-electron

coulomb potential (attraction); $\chi_a(1)$ is a one-electron model spin orbital. Define

one particle model exchange operator:

$$K_b(1) = \int \chi_b^*(2) r_{12}^{-1} \chi_a(2) dx_2 . \qquad (2\text{–}32)$$

$K_b(1)$ is a non-local operator, which has no classic meaning. It is arises from

electron's anti-symmetric nature. Two identical electrons cannot exit in the same

spin orbital. Rewriting the one particle model Fock operator in the form of

coulomb operator and exchange operator gives:

$$f(1) = h(1) + \sum_{b \neq a} J_b(1) - \sum_{b \neq a} K_b(1) \qquad (2\text{–}33)$$

The Hartree-Fock (HF) equation is:

$$f|\chi_a\rangle = \varepsilon_a |\chi_a\rangle \qquad (2\text{–}34)$$

Notice that the Fock operator is a function of the spin orbital, so equation (2-34) is

a pseudo eigenvalue equation, ie. HF equations are non-linear equations needing

to be solved by iterative procedures. The Hartree-Fock Self Consistent Field (HF-

SCF) flow chart is show in Figure 3.

28
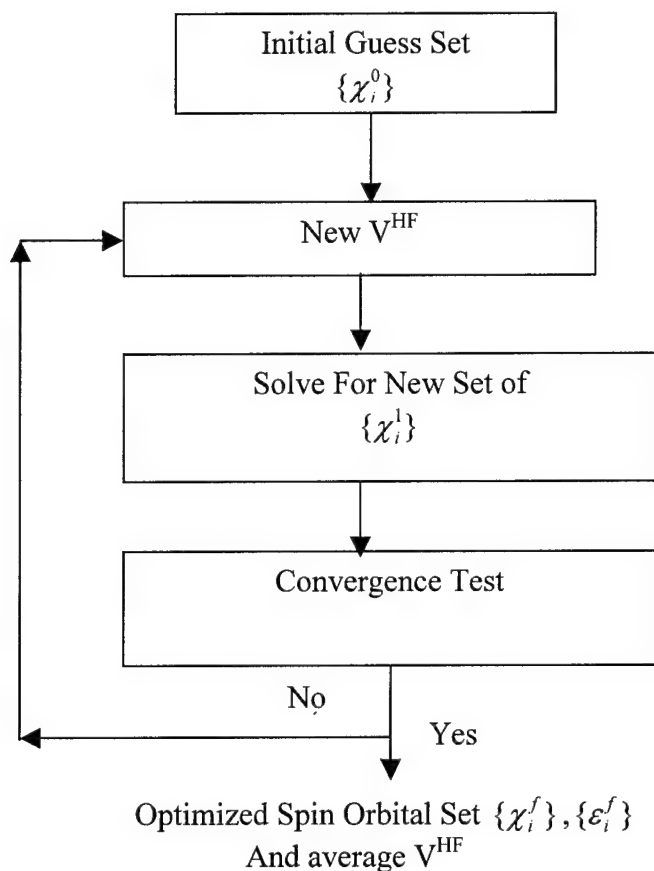
Figure 3. The flow chart of HF-SCF calculation

2.4.2. Closed-Shell Hartree-Fock. Restricted spin orbitals are constructed

to have the same spatial function for both α and β spins. For the closed-shell

Hartree-Fock method, a restricted set of spin orbitals has the form:

$$\chi_i(x) = \{ \begin{array}{l} \psi_j(r)\alpha(\omega) \\ \psi_j(r)\beta(\omega) \end{array} \tag{2–35}$$

and the closed-shell restricted ground state wave function is

$$|\Psi_0\rangle = |\chi_1\chi_2\cdots\chi_{N-1}\chi_N\rangle = |\psi_1\overline{\psi}_1\cdots\psi_a\overline{\psi}_a\cdots\psi_{N/2}\overline{\psi}_{N/2}\rangle \tag{2–36}$$

The general spin orbital HF equation (2–31) is converted to a spatial eigenvalue

equation, where each of the occupied spatial molecular orbitals,

$\{\psi_a | a = 1, 2, \cdots, N/2\}$, is doubly occupied. The sum over all spin orbitals is equal

to the sum over those with spin up and those with spin down:

$$
\begin{aligned}
\sum_a^N \sum_b^N \chi_a \chi_b &= \sum_a^N \chi_a \sum_{\bar{a}}^N \chi_b \\
&= \sum_a^{N/2} (\psi_a + \overline{\psi}_a) \sum_{\bar{a}}^{N/2} (\psi_b + \overline{\psi}_b) \\
&= \sum_a^{N/2} \sum_b^{N/2} \psi_a \psi_b + \psi_a \overline{\psi}_b + \overline{\psi}_a \psi_b + \overline{\psi}_a \overline{\psi}_b
\end{aligned}
\tag{2–37}
$$

Equation (2-28) reduces to an equation involving spatial orbitals; the Hartree-

Fock energy of a closed-shell ground state is:

$$
E_0 = 2 \sum_a^{N/2} (\psi_a | h | \psi_a) + \sum_a^{N/2} \sum_b^{N/2} 2(\psi_a \psi_a | \psi_b \psi_b) - (\psi_a \psi_b | \psi_b \psi_a) \tag{2–38}
$$

or with simplified notation:

$$
E_0 = 2 \sum_a^{N/2} \langle a | h | a \rangle + \sum_{ab}^{N/2} 2 \langle ab | ab \rangle - \langle ab | ba \rangle \tag{2–39}
$$

2.4.3. Solve Hartree-Fock Roothaan Equation. In 1964, Roothaan [14]

used matrix techniques to solve HF equation in restricted spin orbitals (RHF)

case. It can be summarized as following procedure $\{\mathbf{R}_A\}$

1) Specify a molecule (a set of nuclear coordinates, atomic numbers $\{Z_A\}$,

   and number of electrons N) and a basis set $\{\phi_u\}$

2) Calculate all required molecular integrals, S_{uv}, H_{uv}^{core}, and $(uv|\lambda\sigma)$

3) Diagonalize the overlap matrix $\mathbf{S}$ and obtain a transformation matrix $\mathbf{X}$

   Obtain a guess at the density matrix $\mathbf{P}$

4) Calculate the matrix $\mathbf{G}$ of equation from the density matrix $\mathbf{P}$ and the two-electron integrals $(uv|\lambda\sigma)$

5) Add $\mathbf{G}$ to the core-Hamiltonian to obtain the Fock matrix $\mathbf{F} = \mathbf{H}^{core} + \mathbf{G}$

6) Calculate the transformed Fock matrix $\mathbf{F}' = \mathbf{X}^{+}\mathbf{F}\mathbf{X}$

7) Diagonalize $\mathbf{F}'$ to obtain $\mathbf{C}'$ and ε

8) Calculate $\mathbf{C} = \mathbf{X}\mathbf{C}'$

9) Form a new density matrix $\mathbf{P}$ from $\mathbf{C}$ using $P_{uv} = 2\sum_{a}^{\frac{N}{2}} C_{ua}C_{va}^{*}$

10) Determine whether the procedure has converged, ie., determine whether the new density matrix of step (10) is the same as the previous density matrix within a specified criterion. If the procedure has not converged, return to step (5) with the new density matrix.

11) If the procedure has converged, then use the resultant solution, represented by $\mathbf{C}$, $\mathbf{P}$, $\mathbf{F}$, etc., to calculate expectation values and other quantities of interest.

2.4.4. Matrix Element Technique in Roothaan Equation. Since spin has been eliminated, the calculation of molecular orbitals becomes equivalent to the problem of solving the spatial integro-differential equation

$$f(1)\Psi_i(r1) = \varepsilon_i \Psi_i(r1) \tag{2–40}$$

A set of K known basis functions $\{\,\{\phi_u(r)|u=1,2,\cdots,K\}$ is introduced and the

unknown molecular orbitals are expanded in the linear expansion:

$$\psi_i = \sum_{u=1}^{K} C_{ui}\phi_u \qquad\qquad i=1, 2, ..., K \qquad\qquad (2\text{-}41)$$

Using the linear expansion (2-38) by substituting (2-37), one obtains the equation:

$$f_{(1)}\sum_{u=1}^{k} C_{vi}\phi_{u(1)} = \varepsilon_i \sum_{u=1}^{k} C_{ui}\phi_{v(1)}\Phi_{\mu(1)} \qquad\qquad (2\text{-}42)$$

By multiplying both sides by $\phi_u^*(1)$ and integrating it, the integral-differential

equation is turned into a matrix equation:

$$\sum_{v} C_{vi}\int dr_1 \Phi_{u(1)}^* f_{(1)}\Phi_{u(1)} = \varepsilon_i \sum_{v} C_{vi}\int dr_1 \Phi_{u(1)}^* \Phi_{v(1)} \qquad\qquad (2\text{-}43)$$

To solve matrix equation (2-43):

1) Define overlap matrix **S** having elements:

$$S_{uv} = \int \Phi_{u(1)}^* \Phi_{v(1)} dr_1 \qquad\qquad (2\text{-}44)$$

2) Define Fock matrix **F** having elements:

$$F_{uv} = \int \Phi_{u(1)}^* f_{(1)}\Phi_{v(1)} dr_1 \qquad\qquad (2\text{-}45)$$

$$\sum_{v} F_{uv}C_{ui} = \varepsilon_i \sum_{v} S_{uv}C_{vi} \qquad i=1, 2, 3, ...K \qquad\qquad (2\text{-}46)$$

In the form of matrix:

$$\mathbf{F}\,\mathbf{C} = \mathbf{S}\,\mathbf{C}\,\varepsilon \qquad\qquad (2\text{-}47)$$

where **C** is a $K \times K$ square matrix of the expansion coefficients C_{ui}:

$$\mathbf{C} = \begin{pmatrix} C_{11} & C_{12} & ...... & C_{1k} \\ C_{21} & C_{22} & ...... & C_{2k} \\ \vdots & \vdots & \vdots & \vdots \\ C_{k1} & C_{k2} & ...... & C_{kk} \end{pmatrix} \qquad\qquad (2\text{-}48)$$

32

$$
\varepsilon = \begin{pmatrix} \varepsilon_1 & 0 & 0 & 0 \\ 0 & \varepsilon_2 & 0 & 0 \\ 0 & 0 & \ddots & 0 \\ 0 & 0 & 0 & \varepsilon_k \end{pmatrix}
\qquad (2\text{-}49)
$$

The matrix ε is a diagonal matrix of the orbital energies ε_i.

3) The density matrix is defined as:

$$
P_{uv} = 2 \sum_a^{\frac{N}{2}} C_{uv} C_{va}^*
\qquad (2\text{-}50)
$$

If an electron described by the spatial wave function $\psi_a(r)$, then the

probability of finding that electron in a volume element dr at a point r is

$\left| \psi_a(r) \right|^2 dr$. The probability distribution function (charge density) is

$\left| \psi_a(r) \right|^2$. If a closed-shell molecule is described by a single determinant

wave function with each occupied molecular orbital ψ_a containing two

electrons, the total charge density is:

$$
\rho_{(r)} = 2 \sum_a^{\frac{N}{2}} \left| \Psi_a(r) \right|^2
\qquad (2\text{-}51)
$$

$$
= 2 \sum_a^{\frac{N}{2}} \Psi_a^*(r) \Psi_a(r)
$$

$$
= 2 \sum_a^{\frac{N}{2}} \sum_v C_{va}^* \Phi_v^*(r) \sum_u C_{ua} \Phi_u(r)
$$

$$
= \sum_{uv} \left[2 \sum_a^{\frac{N}{2}} C_{ua} C_{va}^* \right] \Phi_u(r) \Phi_v^*(r)
$$

$$
= \sum_{uv} P_{uv} \Phi_u(r) \Phi_v^*(r)
\qquad (2\text{-}52)
$$

Using the Fock operator:

$$\mathbf{f}(1) = \mathbf{h}(1) + \sum_{a}^{\frac{N}{2}} 2\mathbf{J}_a(1) - \mathbf{K}_a(r) \qquad (2\text{-}53)$$

the Fock matrix $\mathbf{F}$ is defined in the basis $\{\Phi_u\}$ with elements:

$$F_{uv} = \int dr_1 \Phi_u^*(1) \mathbf{f}(1) \Phi_v(1)$$

$$= H_{uv}^{core} + \sum_{a}^{\frac{N}{2}} 2(uv|aa) - (ua|av) \qquad (2\text{-}54)$$

$$= H_{uv}^{core} + \sum_{\lambda\delta} P_{\lambda\delta} \left[(uv|\delta\lambda) - \frac{1}{2}(u\lambda|\delta v) \right] \qquad (2\text{-}55)$$

$$= H_{uv}^{core} + G_{uv} \qquad (2\text{-}56)$$

where H^{core} is the one-electron term, which is fixed for a given basis set system; G_{uv} is the two-electron term which depends on the density matrix $\mathbf{P}$ and the two-electron integrals:

$$(uv|\lambda\delta) = \int dr_1 dr_2 \Phi_u^*(1) \Phi_v(1) r_{12}^{-1} \Phi_\lambda^*(2) \Phi_\delta(2) \qquad (2\text{-}57)$$

There are a large number of two-electron integrals to evaluate for HF calculations. This is the major difficulty in Hartree-Fock calculations and all ab initio calculations.

2.4.5. Hartree Fock limit. In the HF calculation, the Fock operator in (2-53) has three terms, the core Hamiltonian $h(1)$, coulomb integral term $\sum_{b \neq a} J_b(1)$

and exchange term $\sum_{b \neq a} K_b(1)$. For this coulomb term, HF method treats the electron as an independent particle, ignoring the electron-electron correlation term. Thus, the use of the uncorrelated electronic wave function in the HF-SCF model will produce larger errors for chemical reactions that involve bond making

and breaking compared to the calculation of equilibrium properties. Increasing

the size of the basis set may improve HF-SCF answer, which will converge to a

limit, the so-called Hartree-Fock limit. The correlation energy is defined as the

difference between the exact energy and the energy at the Hartree-Fock limit:

$E_{correlation} = E_{exact} - E_{HF}$. The correlation energy at equilibrium is typically 20-30%

of the dissociation energy, ie., the correlation errors are large.

2.5 Post Hartree-Fock Calculations

2.5.1 Configuration Interaction (CI). The basic idea is to diagonalize the

N-electron Hamiltonian in a basis of N-electron functions (Slater determinants),

ie., represent the exact wave function as a linear combination of N-electron trial

functions and use the linear variational method. If the basis were complete, one

would obtain the exact energies not only of the ground state but also of all excited

states of the system. In principle, CI provides an exact solution for many-electron

problems. In practice, however, one only can handle a finite set of N-electron

trial functions; consequently, CI provides only upper bounds to the exact energies.

One way to construct determinantal trial functions are to use weighted sums of

Hartree-Fock molecular orbitals obtained by solving Roothaan's equations. The

form of full CI wave function can be written as:

$$|\Phi_0\rangle = c_0|\Psi_0\rangle + \sum_{ar} c_a^r|\Psi_a^r\rangle + \sum_{\substack{a<b \\ r<s}} c_{ab}^{rs}|\Psi_{ab}^{rs}\rangle$$

$$+ \sum_{\substack{a<b<c \\ r<s<t}} c_{abc}^{rst}|\Psi_{abc}^{rst}\rangle + \sum_{\substack{a<b<c<d \\ r<s<t<u}} c_{abcd}^{rstu}|\Psi_{abcd}^{rstu}\rangle + \cdots \qquad (2\text{-}58)$$

Where $|\Phi_0\rangle$ is the exact many-electron wave function, $|\Psi_0\rangle$ is a reasonable approximation to $|\Phi_0\rangle$, $|\Psi_a^r\rangle$ is a possible singly excited determinants (which differ from $|\Psi_0\rangle$), $|\Psi_{ab}^{rs}\rangle$ is the doubly excited determinants, etc., and c_a^r is the relevant coefficient of excited determinants.

Given the trial function of Equation (2-46), one can find the corresponding energies by using the linear variational method. The lowest eigenvalue will be an upper bound to the ground state energy of the system. The higher eigenvalues will be upper bounds to excited states for the system. The difference between the lowest eigenvalue and the Hartree-Fock energy obtained within the same one-electron basis is called the basis set correlation energy. As the one-electron basis set approaches completeness, this basis set correlation energy approaches the exact correlation energy. For a given one-electron basis set, full CI is the best one can do.

2.5.2. Multi-configuration self-consistent field (MCSCF) calculation.

The canonical Hartree-Fock orbitals are not the best choice of orbitals for use in CI calculation. Consider a multi-determinantal wave function, containing a relatively small number of configurations, and vary these orbitals so as to minimize the energy. This is called the multi-configuration self-consistent field (MCSCF) method. The MCSCF wave function is a truncated CI expansion:

$$|\Psi_{MCSCF}\rangle = \sum_I c_I |\Psi_I\rangle \tag{2-59}$$

in which both the expansion coefficients (c_I) and the orthonormal orbitals contained in $|\Psi_I\rangle$ are optimized. The general equations are more complicated than Roothaan's restricted Hartree-Fock equation. The result is much closer to the exact solution.

2.5.3. The completed active space (CAS) calculation.

CAS combines the SCF computation with a full CI involving with a subset of orbitals, which is known as the active space. It is a very high-level ab initio calculation method.

2.6 Semi-empirical HF-SCF Method (AM1)

In order to calculate larger molecules inexpensively, additional approximations are required beyond those used in the ab initio method. The most difficult and time-consuming procedure of the ab initio method is the computation of the large number of two electron (repulsion or exchange) integrals, such as the matrix elements in Equations (2-44), (2-45), (2-46). One important fact is that the overlap between different atomic orbitals of an electronic model usually is very small, and can be approximately neglected. For example, the overlap between 1s and 2p orbitals from the same atom is essentially zero. The overlap between two different atomic orbitals describing the molecular orbital of an electron is referred as differential overlap (DO). If the atomic orbitals originate from the same atom, it is called monatomic differential overlap; if from different atoms it is called diatomic differential overlap. By assuming differential overlap to be negligible, a large number of integrals involved in the Fock operator can be set to zero. This

neglect of differential overlap (NDO) formed the basis for the first semi-empirical

method. According to the approximation level, there are various models, such as,

completed neglect of differential overlap (CNDO); intermediate neglect of

differential overlap (INDO), neglect of diatomic differential overlap (NDDO);

modified neglect of diatomic overlap (MNDO). The Austin Model 1 (AM1)

semi-empirical Hamiltonian method was used in this thesis. AM1 is an extension

of the earlier version of MNDO/3 Hamiltonian. In attempted to correct MNDO's

deficiency by assigning a number of spherical Gaussian functions to each atom to

mimic correlation effects [22]. The flow chart of AM1 SCF calculation is showed

in Figure 4.

```
        ┌──────────────────────────┐
        │ Initial Guess of Geometry │
        └──────────────────────────┘
                     │
                     ▼
          ┌───────────────────┐
          │ Assign Parameters  │
          └───────────────────┘
                     │
                     ▼
          ┌───────────────────┐
    ┌────▶│  SCF Calculation   │
    │     └───────────────────┘
    │                │
    │               │ Yes
┌─────────┐   No  ┌───────────┐
│  New    │◀──────│  Energy   │
│Geometry │       │ Converge  │
└─────────┘       └───────────┘
                     │
                     ▼
                  Result
```
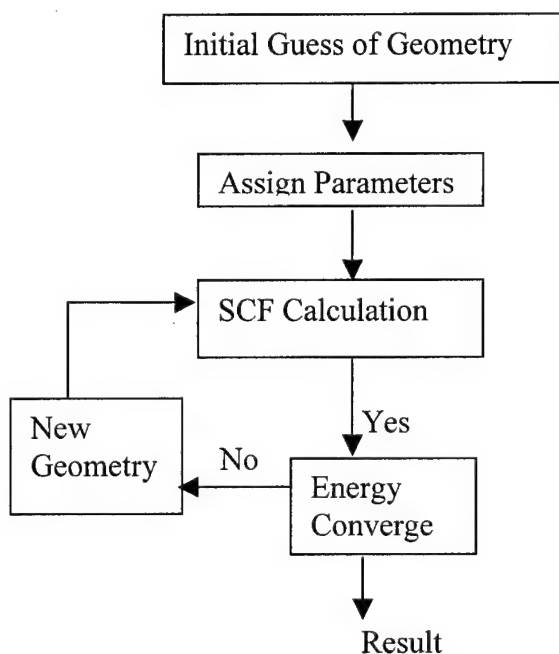
Figure 4. The flow chart of AM1-SCF calculation

Another simplification in the SE method is to treat interaction integrals as element-specific parameters. The number of parameters required to describe an element corresponds to the number of interaction terms in the approximate Hamiltonian used. Examples of parameters are the one-electron energy of an atomic orbital of an ion (bare nucleus + core electrons) resulting from the removal of all valence electrons, an atomic Slater orbital exponent, or the exponent in Gaussian describing core-core repulsion. The ultimate success of the SE method hinges on the validity of the approximate Hamiltonian used and on the values of the parameters used. Ideally, one would want the parameters that describe each element to be completely independent of the molecular environment. In reality, the specific molecular environment does affect the atomic parameters. In order to make the application of the method generic, the parameters are selected to minimize the least square error for selected molecular properties for a large set of molecules. In accepting experimental parameters the variational principle is no longer valid.

It should be noted that the use of experimental data to determine the parameters in SE method results in chemical usefulness and efficiency. Because SE can significantly reduced the computational time, it can be applied to large systems, such as bulk materials, surface modeling, and polymer calculations. In some case, SE can predict the better results than Hartree-Fock ab initio methods. However, to improve the agreement with the experiment, more terms are added to the approximation model, consequently, the physical meaning of each term

becomes more poorly defined and SE technique becomes more of a curve fit than

a physical model. Complete discussions of SE methods see reference [23].

2.7 Density Functional Theory (DFT)

2.7.1. Basic Principle of DFT Method. Many body quantum problems can

be rigorously recast in the form of an auxiliary single-body problem. Ground

state observable are uniquely determined by ground state electron density, ρ.

Observables, like energy, are a function of the ground state electron density. In

DFT theory, the particle-particle interactions are represented as a density-

dependent single-particle potential. In this potential are included direct (Hartree)

contribution and exchange-correlation part, which is a functional of electron

density. The exact density functional is unknown, so the objective of DFT is to

derive simple approximations to the density functional (DF).

The standard approximation for the exchange-correlation energy functional

(X-C) is the local density approximation (LDA). The true X-C energy density is

replaced by the X-C energy density of an electron gas.

2.7.2. A Simplified Derivation of DFT Theory.

$$E_t(\rho) \quad = \quad T(\rho) \quad + \quad U(\rho) \quad + \quad E_{xc}(\rho) \qquad (2\text{-}60)$$

$E_t(\rho)$ is the total energy of a system where $T(\rho)$, the kinetic energy of a

system of non-interacting particles is a function of density ρ. $U(\rho)$ is the classical

electrostatic energy due to columbic interaction. $E_{xc}(\rho)$ is an interaction includes

all many-body contribution to the total energy, in particular the exchange and correlation energies the exact form of which is not known.

Choose an orthogonal basis set, then:

$$\langle \psi_i | \psi_j \rangle = \delta_{ij} \tag{2-61}$$

The charge density is given as:

$$\rho(r) = \sum_i |\psi_i(r)|^2 \tag{2-62}$$

$$T = \sum_i^N \langle \psi_i | -\frac{1}{2}\nabla^2 | \psi_i \rangle \tag{2-63}$$

$$U = \sum_i^n \sum_\alpha^N \langle \Phi_{i(r)} \left| \frac{-Z}{R_\alpha - r} \right| \Phi_{i(r)} \rangle$$

$$+ \frac{1}{2}\sum_i \sum_j \langle \Phi_{i(r1)}\Phi_{j(r2)} \frac{1}{r_1 - r_2} \Phi_{i(r1)}\Phi_{j(r2)} \rangle$$

$$+ \sum_\alpha^N \sum_{\beta \angle \alpha} \frac{Z_\alpha - Z_\beta}{R_\alpha - R_\beta} + \sum_\alpha^N \sum_{\beta \angle \alpha} \frac{Z_\alpha - Z_\beta}{R_\alpha - R_\beta}$$

$$= \varepsilon \mathbf{S}^* \mathbf{C} \sum_\alpha^N \langle \rho_{(r1)} \frac{Z_\alpha}{|R_\alpha - r|} \rangle + \frac{1}{2}\langle \rho_{(r1)}\rho_{(r2)} \frac{1}{|r_1 - r_2|} \rangle + \sum_\alpha^N \sum_{\beta \angle \alpha} \frac{Z_\alpha Z_\beta}{|R_\alpha - R_\beta|}$$

$$= <-\rho(r_1)V_N> \quad + \quad <\rho(r_1)\frac{V_e(r_1)}{2}> \quad + \quad <V_{NN}> \tag{2-64}$$

electron-nucleus   electron-electron   nucleus-nucleus

$E_{xc}(\rho)$ is usually separated into exchange and correlation functional components which are local or non-local in density, ie.:

$$E_{xc}(\rho) = \int \varepsilon_{xc}[\rho(r)] \rho(r)dr \tag{2-65}$$

41

$$\varepsilon_{xc}(\rho) = \varepsilon_x(\rho) \quad + \quad \varepsilon_{x,NL}(\rho, \nabla\rho) \quad + \quad \varepsilon_c(\rho) + \quad \varepsilon_{c,NL}(\rho, \nabla\rho)$$

$$(2\text{-}66)$$

exchange local	exchange non-local	correlation local	correlation non-local

$\varepsilon_{xc}(\rho)$ is exchange-correlation energy per particle in a uniform electron gas.

2.7.3. Local Density Approximation (LDA).

LDA assumes that the charge density varies slowly on an atomic scale (i.e. each region of a molecule actually looks like a uniform electron gas) and the non-local functional components $\varepsilon_{x,NL}(\rho, \nabla\rho)$ and $\varepsilon_{c,NL}(\rho, \nabla\rho)$ can be ignored. In this paper, LDA was applied. For detailed discussions and the presentation of the non-local density approximation (NLDA) please see reference [24].

2.7.4. Beck's Three-Parameter Hybrid Functional.

Using LYP Correlation Functionals, there are a lot of functionals from which to choose to serve individual application purposes. Based on SiC cluster results from previous calculations [14], we choose Beck 3LYP type functional [25]. It has the form of:

$$A*Ex^{Slater} + (1-A)*Ex^{HF} + B*\}Ex^{Becke} + Ec^{VWM} + C*\}Ec^{non\text{-}local} \qquad (2\text{-}67)$$

The non-local correlation is provided by the LYP expression, and VWN is functional III (not functional V) [26], the constants A, B, and C are those determined by Beck by fitting to the G1 molecule set.

2.7.5. Computation Process.

Similar to HF calculation, the matrix elements were employed to calculate the energies in which we are interested; the first step is to write the total energy expression as:

$$E_t(\rho) = \sum_i \left\langle \Phi_i \left| -\frac{\nabla^2}{2} \right| \Phi_i \right\rangle + \left\langle \rho_{(r1)} \left(\varepsilon_{xc}(\rho_{(r1)}) + \frac{V_{e(r1)}}{2} - V_N \right) \right\rangle + V_{NN} \quad (2\text{-}68)$$

To minimizing E_t with respect to ρ, subject to the orthonormality constraints [27], the following term is set to zero:

$$\frac{\partial E_t}{\partial \rho} - \sum_i \sum_j \varepsilon_{ij} \left\langle \Phi_i | \Phi_j \right\rangle = 0 \quad (2\text{-}69)$$

where ε_{ij} are Lagrange Multipliers. Then, the Kohn-Sham Equation is:

$$\left\{ -\frac{\nabla^2}{2} - V_n + V_e + u_{xc}(\rho) \right\} \Phi_i = \varepsilon_i \Phi_i \quad (2\text{-}70)$$

$$u_{xc} = \frac{\partial}{\partial \rho}(\rho \varepsilon_{xc}) \quad (2\text{-}71)$$

where u_{xc} is a universal functional of electron density. This step is similar to HF's initial guess for the wave function. Then the total energy including exchange and correlation term is a function of electron density:

$$E_t = \sum_i \varepsilon_i + \left\langle \rho_{(r1)} \left(\varepsilon_{xc}(\rho) - u_{xc}(\rho) - \frac{V_{e(r1)}}{2} \right) \right\rangle + V_{NN} \quad (2\text{-}72)$$

A local combination atomic orbital approximation solution results from the following choice of wave function form:

$$\Phi_i = \sum_u C_{iu} \chi_u \quad (2\text{-}73)$$

where χ_u is the spin orbital wave equation just like in the HF-Roothaan equation. In the matrix form:

43

$$\mathbf{H\,C} = \varepsilon\,\mathbf{S\,C} \tag{2-74}$$

The **H** matrix elements are given as:

$$[-\frac{\nabla^2}{2} + V_c(r) + u_x^i(r)]\psi_i = \varepsilon_i\psi_i$$

$$[-\frac{\nabla^2}{2} + V_c(r) + u_{xc}(r)]\psi_i = \varepsilon_i\psi_i \tag{2-75}$$

$$\mathbf{H}_{uv} = \left\langle \chi_{u(r1)} \left| -\frac{\nabla^2}{2} - V_N + V_e + u_{xc}(\rho) \right| \chi_{v(r1)} \right\rangle \tag{2-76}$$

The **S** matrix elements are:

$$\mathbf{S}_{uv} = \left\langle \chi_{u(r1)} | \chi_{v(r1)} \right\rangle \tag{2-77}$$

The DFT calculation process first evaluates $u_{xc} = \dfrac{\partial}{\partial\rho}(\rho\varepsilon_{xc})$, the universal

electron density functional, then other steps are very similar to solving HF-

Roothaan equation. Because of this extra term, DFT calculations are more

expensive than HF calculations. However, DFT calculations included both

exchange and correlation terms, which the HF calculation ignores. Therefore,

comparable DFT calculations are more accurate than HF calculations. The SCF

calculation process is shown in Figure 5 below.

$$\rho^{in}(r)$$

$$-\frac{1}{2}\nabla^2 V_c(r) = 4\pi\rho(r)$$

$$u_{xc}(r) = f[\rho(r)]$$

$$[-\frac{\nabla^2}{2} + V_c(r) + u_{xc}(r)]\psi_i = \varepsilon_i\psi_i$$

$$\psi_i = \sum_p C_{ip}\Phi_p$$

$$(H_{pq} - \varepsilon_i S_{pq})C_{iq} = 0$$

$$H_{pq} = \int \Phi_p^*(r)[-\frac{\nabla^2}{2} + V_c(r) + u_{xc}(r)]\Phi_q(r)dr$$

$$S_{pq} = \int \Phi_p^*(r)\Phi_q(r)dr$$

$$\partial E/\partial\rho = 0$$
$$\rho^{out}(r) = \sum_{occ}|\psi_i(r)|^2$$

$$E = E[\rho, R_\alpha]$$

$$\partial E / \partial R_\alpha$$
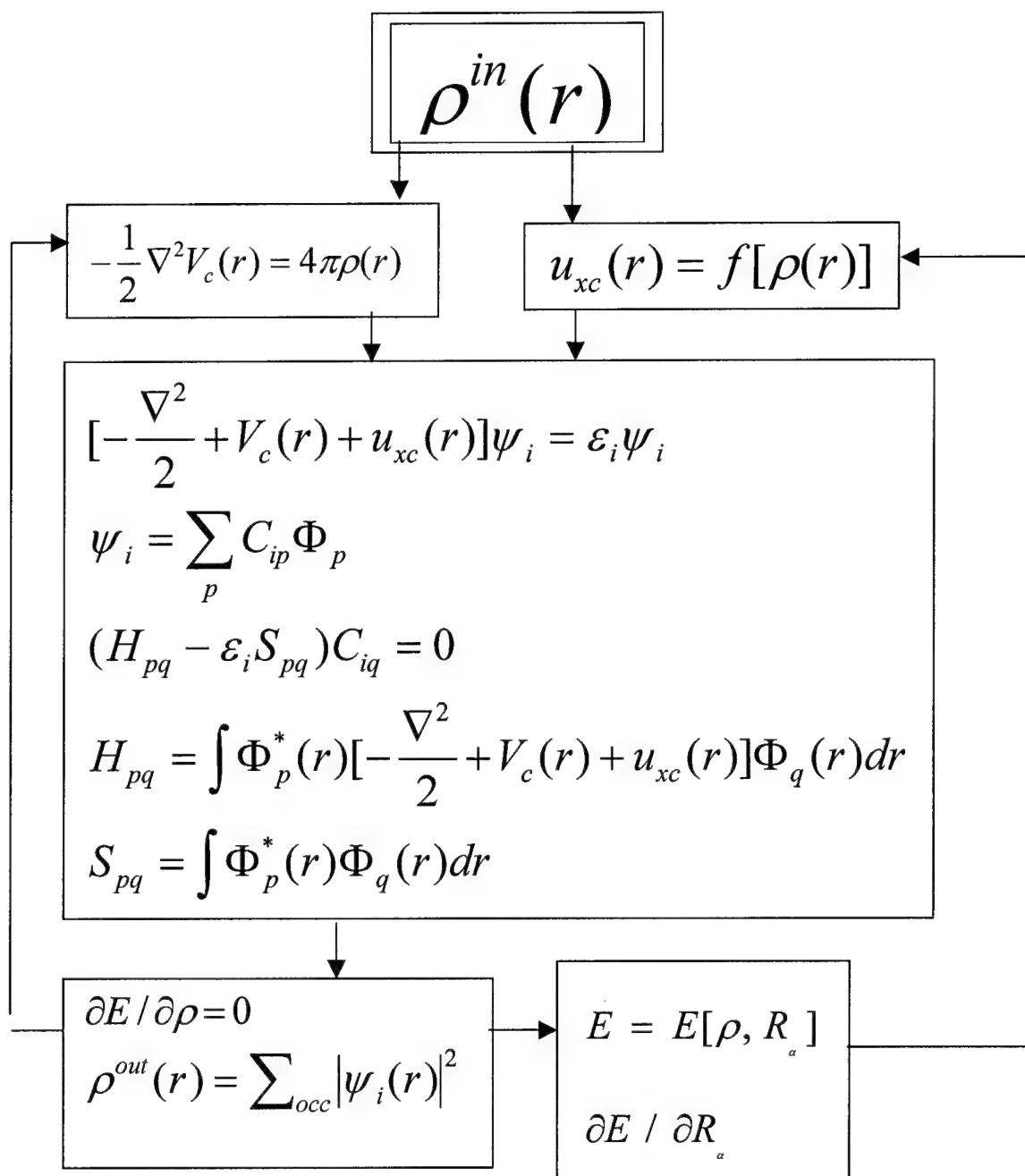
Figure 5. The flow chart of DFT-SCF calculation

45

A brief comparison of HF method and DFT method equations follow:

HF (1928, 1930)   DFT (1964, 1965)

$$E = E[\Psi, R_\alpha]$$ (1a) $$E = E[\rho, R_\alpha]$$ (1b)

$$E = \int \Psi^* [\sum_i h_i + \sum_{i>j} \frac{1}{r_{ij}}] \Psi d\tau$$ (2a) $$E = T(\rho) + U(\rho) + E_{xc}(\rho)$$ (2b)

$$\Psi = |\psi_1(1), \psi_2(2), \cdots \psi_n(n)|$$ (3a) $$\rho(r) = \sum_{occ} |\psi_i(r)|^2$$ (3b)

$$\partial E / \partial \Psi = 0$$ (4a) $$\partial E / \partial \rho = 0$$ (4b)

$$[-\frac{\nabla^2}{2} + V_c(r) + u_x^i(r)]\psi_i = \varepsilon_i \psi_i$$ (5a) $$[-\frac{\nabla^2}{2} + V_c(r) + u_{xc}(r)]\psi_i = \varepsilon_i \psi_i$$ (5b)

The explanation of these equations follows:

1a: Total energy is expressed as a function of total wave function

1b: Total energy is written as a function of total electron density

2a: Total energy is an expectation value of the exact Hamiltonian

2b: Total energy is decomposed in a formally exact way into three terms

3a: Total wave function is approximation zed by Slater determinant

3b: Total density is decomposed into single-particle density that originates from one particle wave function

4a: Variational principle applied to the Slater determinant

4b: Variational principle applied to the total electron density

5a: Hartree-Fock Equation: One particle eigenvalue equation

5b: Kohn-Sham Equation: One particle effective Schrödinger equation

III. Assessment of Accuracy of AM1 Method for Silicon Carbide System

All AM1 calculations were carried out using a Sgi O2 workstation, which has IRX 6.5 operating system. The software package of GAMESS version 10 Jan 2000 is used for AM1 calculations. The initial geometric coordinates were obtained from HyperChem 4.0 AM1/MM calculation on Pentium 200. Restricted open shell calculations (ROHF) were used for all calculations.

As a semi-empirical method, AM1 has the advantage of being fast. On the other hand, it has the disadvantage of poorly predicting geometries for molecules different from those used to determine parameters. Similarly, SE methods can predict the energies close to the experiment results, when they are parameterized with both experimental energies and structures that are similar to those used to derive parameters. Following is a comparison study on Si_mC_n clusters (m + n =4, 5, 6, 7, 8) using AM1 method with DFT method and experiment results.

3.1 Comparison Study of Si_2C_3 Isomers Using AM1, HF and DFT Methods

Six linear and eight non-linear Si_2C_3 isomers are found with singlet (S_0) and triplet (T_0) minimum energy optimization using HF and DFT calculation [see 14]. These structures are showed in Figure 6.
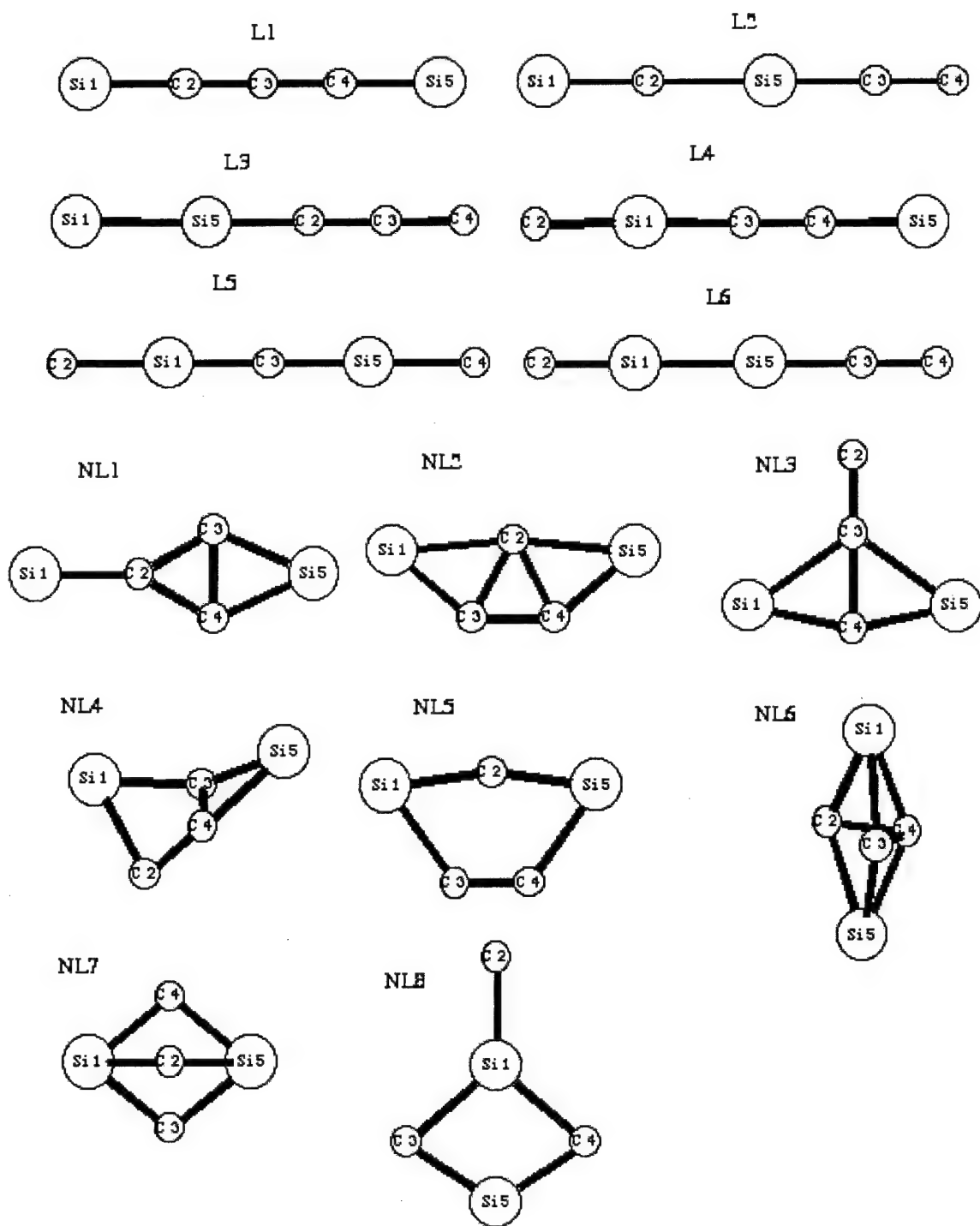
Figure 6. The structures of Si$_2$C$_3$ isomers predicted by HF and DFT methods

48

Six linear and six non-linear Si_2C_3 isomers are found with singlet (S_0) and triplet (T_0) minimum energy optimization using AM1 method. The nonlinear structures are showed in Figure 7
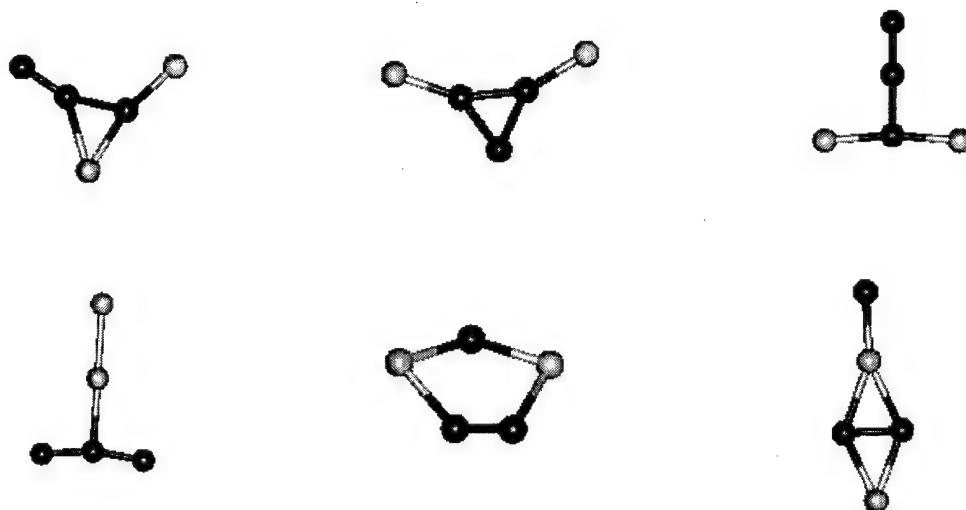
Figure 7. The non-linear Si_2C_3 isomers structures predicted by AM1 method

Comparing the listed structure in Figure 6 and Figure 7, the linear structures predicted by AM1 method are similar to the linear structures predicted by HF and DFT method, but with different bond lengths. The bond lengths of linear structure of Si_2C_3 isomers are listed in Table 5. For nonlinear structures, the AM1 method only predicts that there are six nonlinear structures for Si_2C_3 isomers (see Figure 7), but HF and DFT method predict that there are eight nonlinear structures for Si_2C_3 isomers (see Figure 6). Comparing Figure 6 and Figure 7, AM1 method is not able to predict the three-dimensional structures of Si_2C_3 isomers.

Table 5. The bond length comparison for linear Si_2C_3 isomers calculations using by different methods

Isomer		Bond Length Parameters					
		AM1		HF*		DFT*	
		S_0	T_0	S_0	T_0	S_0	T_0
L1	Sym.	$D_{\infty h}$	$C_{\infty h}$	$D_{\infty h}$	$D_{\infty h}$	$D_{\infty h}$	$D_{\infty h}$
	Si_1-C_2	1.552	1.511	1.672	1.739	1.704	1.763
	C_2-C_3	1.276	1.318	1.287	1.282	1.297	1.296
	C_3-C_4		1.242				
	$C4-C5$		1.587				
L2	Sym.	$C_{\infty h}$	$C_{\infty h}$	$C_{\infty h}$	$C_{\infty h}$	$C_{\infty h}$	$C_{\infty h}$
	Si_1-C_2	1.555	1.549	1.671	1.866	1.695	1.750
	C_2-Si_5	1.533	1.544	1.649	1.670	1.675	2.024
	Si_5-C_3	1.549	1.552	1.667	1.667	1.687	1.750
	C_3-C_4	1.260	1.261	1.262	1.264	1.282	1.293
L3	Sym.	$C_{\infty h}$	$C_{\infty h}$	$C_{\infty h}$	$C_{\infty h}$	$C_{\infty h}$	$C_{\infty h}$
	Si_1-Si_5	1.977	1.918	2.127	2.156	2.169	2.233
	Si_5-C_2	1.597	1.592	1.717	1.760	1.718	1.725
	C_2-C_3	1.279	1.277	1.278	1.248	1.294	1.291
	C_3-C_4	1.283	1.287	1.285	1.341	1.304	1.317
L4	Sym.	$C_{\infty h}$	$C_{\infty h}$	$C_{\infty h}$	$C_{\infty h}$	$C_{\infty h}$	$C_{\infty h}$
	Si_1-C_2	1.581	1.565	1.702	1.719	1.745	1.772
	Si_1-C_3	1.249	1.255	1.751	1.783	1.748	1.761
	$C3-C_4$	1.639	1.625	1.251	1.223	1.274	1.263
	C_4-Si_5	1.574	1.580	1.714	1.847	1.740	1.793
L5	Sym.	$D_{\infty h}$	$D_{\infty h}$	$D_{\infty h}$	$C_{\infty h}$	$D_{\infty h}$	$D_{\infty h}$
	Si_1-C_2	1.609	1.629	1.791	1.800	1.770	1.806
	Si_1-C_3	1.603	1.536	1.660	1.658	1.700	1.698
	C_3-Si_5				1.652		
	Si_5-C_4				1.823		
L6	Sym.	$C_{\infty h}$	$C_{\infty h}$	$C_{\infty h}$	$C_{\infty h}$	$C_{\infty h}$	
	Si_1-C_2	1.588	1.491	1.594	1.846	1.743	
	Si_1-Si_5	2.010	2.242	2.074	2.102	2.162	
	Si_5-C_3	1.535	1.544	1.679	1.672	1.689	
	C_3-C_4	1.278	1.280	1.267	1.269	1.290	

*Other than AM1 method are calculated by Duan[14].

Observing Table 5, one can see that AM1 predicts the shortest bond lengths among these three methods. For the same symmetry structure, NL6, in singlet

optimization, for the bond length between Si_1 and C_2 (see Fig. 6 and Table 5) AM1 predicts 1.588 Å, HF predicts 1.594Å, and DFT predicts 1.743Å. By comparing all bond length listed in the Table 5, one can see that the order of bond length by different calculation methods is: AM1 < HF < DFT. There are only a few exceptions, such as the C_3-C_4 bond length in structure L4, where AM1 predicts larger bond length than HF by 0.40 Å and larger than DFT by 0.36 Å; and the C_3-C_4 bond length in structure L6, where AM1 predict larger bond length than HF by 0.01 Å. The DFT method predicts average bond length larger than AM1 method by 0.165 Å, and the HF method predicts average bond length larger than AM1 method by 0.139 Å.

Besides the differences in bond lengths, AM1 is not able to predict NL6 and NL4, the three-dimensional structures found using HF and DFT methods. Because AM1 predicts the bond lengths too short, the repulsion forces are too high in three-dimensional structures. However, all above three methods, AM1, HF, and DFT are agreed that L1 is the ground state structure.

The electron affinity results calculated by several methods are listed in Table 6 [14] (see next page). Results show that the DFT method using large basis set (cc-pV5Z+) predicts the best result for electron affinity, which is excellent agreement with the experimental result. Notice that AM1 predicts a better result than HF method, and DFT method using medium basis set (cc-pVDZ).

Table 6. A comparison of electron affinity results of Si_2C_3 cluster using different method with experiment result

Calculation	S_0	T_0	D_0	EA[*]
AM1	0.000	1.653	-1.572	1.572
HF/cc-pVDZ	0.000	0.904	-0.675	0.637
B3LYP/cc-pVDZ	0.000	0.530	-1.474	1.512
B3LYP/cc-pV5Z+// B3LYP/cc-pVDZ	0.000	-	-1.704	1.742
Experiment[**]				1.769

Other than AM1 method are conducted by Duan [14]

*EA$= \Delta E(S_0 - D_0) + \Delta ZPE(S_0 - D_0)$
**Reference [15]

Comparing the calculation results with experiment results, the HF method predicts a very poor result. At the medium basis set level cc-pVDZ, both DFT and HF method predictions for electron affinity are less accurate result than the AM1 method. As basis sets increased up to cc-pV5Z+, DFT gives more accurate result than both AM1 and HF method. The absolute error of DFT method in electron affinity calculation is 0.027 eV, which is excellent agreement with the experiment result.

As a semi-empirical method, AM1 is very efficient. During the geometry optimization calculation of Si_mC_n (m + n = 6) clusters, the AM1 method takes only about a few minutes to finish a single geometry optimization calculation. It takes HF method 2 hours, and it takes the DFT method more than 10 hours to do it. A question is raised, why SE AM1 method gives better electron affinity results than HF method in calculation? Because in the HF approximation, the correlation

energy had been ignored (see chapter 2, section 2.4.6), as a result, HF always has poor performance in calculation of electron affinity. As a semi-empirical method, AM1 is parameterized by experiment data, such as energies. Thus it is not surprising that the SE method gives a result close to the experiment results.

On the other hand, HF and DFT predict more accurate geometries than the AM1 method. As a SE method, AM1 is parameterized in a way that lacks flexibility to model SiC systems, so the bonding predicting in AM1 is too short in the SiC system. The SE method does not have flexibility of user assigned basis sets, so the basis sets are small (AM1 and most SE methods use a "minimum basis set"), and there is no possibility to add diffuse functions to the basis set. For the SiC cluster system, Si atom is big and polarizable. It normally requires adding diffuse function to the basis functions, so the SE AM1 method fails.

3.2 Study Si_mC_n Cluster Structures (m+n = 6) Using AM1 Method

In order to assess the AM1 method more carefully, we studied the predicted structures for Si_mC_n cluster (m+n=6) with singlet and triplet energy optimization using AM1 method. The structures of isomers are listed in Figure 8 (see next page). Structures #1 through #7 are shown in order of increasing energy. Other structures than #7 are not included in this paper, because their energy is too high. The detailed energy data are listed in the Appendix B. During optimizing, it is observed the structures of singlet states and the triplet states are very similar, so they will not be separately displayed.
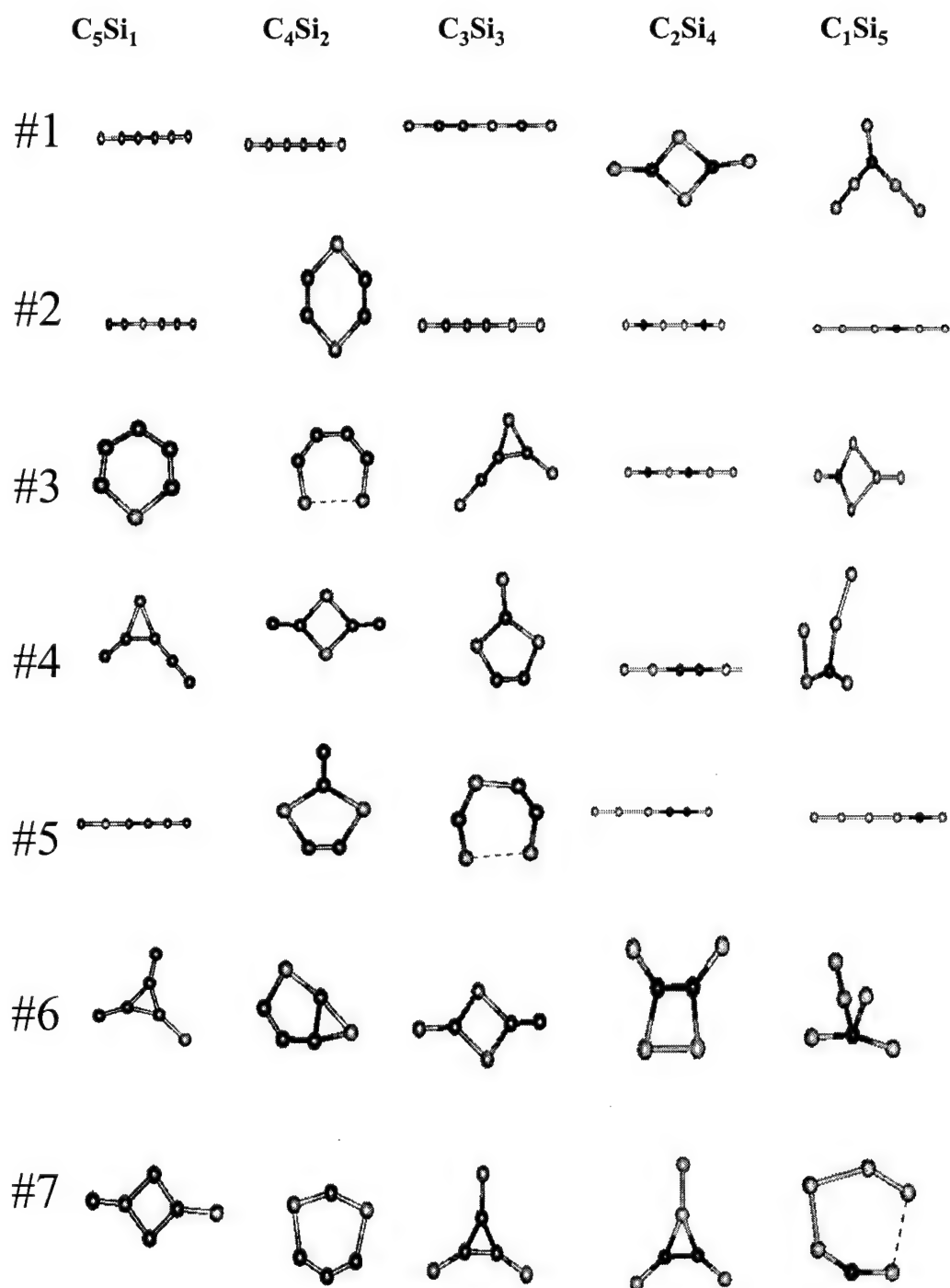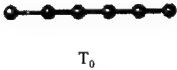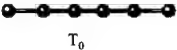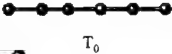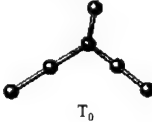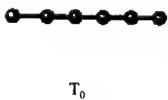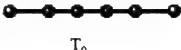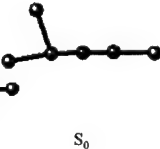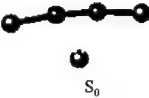
Figure 8. The structures of Si_mC_n clusters predicted by AM1 method

54

Observing Figure 8, one can conclude that:

1) The lowest energy singlet and triplet structures tend to be linear, when number of silicon atoms less than or equal to 3, recalling the properties of pure C clusters. Pure Si clusters tends to form the three-dimensional structure, and pure C tends to form the linear structure. With the number of Si atom increasing in Si_mC_n cluster, the mixed clusters are expected to show pure Si cluster characteristics, such as tendency toward non-linear structure. On the other hand, when C atoms are the majority in the cluster molecule, the cluster tends to from the linear structure characteristic of pure C clusters.

2) For AM1 calculations of #6 structure of Si_3C_3 and #5 structure of Si_2C_4 triplet structure energies are lower than singlet energies. The difference between singlet energy and triplet energy is about 0.1 eV for #6 structure of Si_3C_3, about 0.6 eV for #5 structure of Si_2C_4. It might be true that AM1 tends to favor triplet energy state. Another interpretation is that AM1 method does not have enough flexibility, so it treats different clusters in the same manner.

3) Lowest energy structures minimize the number of weak Si-Si bonds, and then minimize the number of Si-C bonds. Si atoms go to terminal positions. C-C bonding is strong bonding, and C atoms are found to be multi-bonded.

   For the ground state structures (#1 structures), compare to the ground

structure and electron affinities of same clusters predicted by DFT method and experimental results are shown in Figure 9.

	C_5Si_1	C_4Si_2	C_3Si_3	C_2Si_4	C_1Si_5
AM1 EA (eV)	3.335	1.135	2.280	1.381	-0.0142
DFT EA (eV)	3.09	2.38	2.30	0.96	1.27
Experimental EA (eV)		2.56			

Figure 9. A comparison of AM1 predictions, DFT predictions and experimental result for Si_mC_n clusters (m+n=6)

Looking at Figure 9, one can see that the AM1 method and DFT method predict different ground state structures for SiC clusters. Both methods predict the SiC clusters have bent structures as the Si atoms increase to more than 3 atoms. AM1 predicts all 5 structures in Figure 9 are in triplet state, DFT method predicts there are 3 molecules in singlet states and two molecules in triplet states. Comparing the calculation results of AM1 method and DFT method to experimental results, the DFT method gives more accurate results.

3.3 Comparison of AM1 Calculations and DFT Calculations with Experimental Results for Si_mC_n Clusters (m+n=4,5,6,7,8)

To estimate the reliability of AM1 calculation, a more complete comparison study is performed for Si_mC_n clusters range from m+n=4 to 8. The comparison subjects include geometry optimization, electron affinity calculations and vibration frequency calculations using AM1 method and DFT method compared with experimental results. The detailed data are listed in the Table 7. The AM1 method and DFT method both predict the same structures that experimental results show. However, the DFT method provides more accurate and more reliable results than the AM1 method does. The root mean square error of electron affinity calculation by DFT method has negative offset 0.1 eV, and AM1 method has 0.728 eV negative offsets. The electron affinity calculation results and the experimental results from Table 7 are plotted in Figure 10.

By looking at the Figure 10, one can see that the DFT method predicts the exact same electron affinity tendency as the experimental results, while AM1 method predictions oscillate badly back and forth. For AM1, there are two very bad results among 6 clusters. One bad result came from Si_3C cluster, AM1 predicts it has triplet ground state but DFT predicts it has singlet ground state structure.

Table 7. A comparison of AM1 and DFT calculations with experimental results for Si_mC_n clusters (m+n=4, 5, 6, 7, 8)

Cluster		Si_3C	SiC_3	SiC_4	Si_2C_3	Si_2C_4	Si_2C_5
Expt. Structure		Rhombic	Linear	Linear	Linear	Linear	Linear
AM1 Prediction		Rhombic T_0	Linear T_0	Linear S_0	Linear S_0	Linear T_0	Linear T_0
AM1 Energy (eV.)	S_0	0.0000	0.000	0.000	0.000	0.000	0.000
	T_0	-0.984	-0.959	-0.294	1.817	-1.137	1.619
	D_0	-1.771	-3.889	-2.136	-1.573	-2.101	-2.116
AM1 EA (eV)		**0.786**	**2.926**	**2.134**	**1.572**	**0.963**	**2.114**
AM1 Freq. (cm^{-1})	f_1	336		584	329	591	65
	f_2	368	1577	1356	1103	1000	343
	f_3		2207	2078	1835	1835	2311
Expt. Freq. (cm^{-1})	f_1	315	1950	565	420	845	40
	f_2	490	2015	1105	910	1175	340
	f_3		2185	2120	1860	1860	
Expt. EA (eV)		**1.535**	**2.839**	**2.327**	**1.769**	**2.556**	**2.136**
AM1 EA Error		-0.749	0.087	-0.193	-0.197	-1.593	-0.022
Error (cm^{-1})	f_1	-21	438	-19	91	254	-25
AM1 Error (cm^{-1})	f_2	122	-22	-251	-193	175	-3
AM1 Error (cm^{-1})	f_3			-218	-350	25	
DFT EA (eV)		**1.491**	**2.694**	**2.285**	**1.684**	**2.378**	**2.087**
DFT Error (eV)		**-0.044**	**-0.147**	**-0.042**	**-0.085**	**-0.178**	**-0.049**

Error = calculation result – experimental result
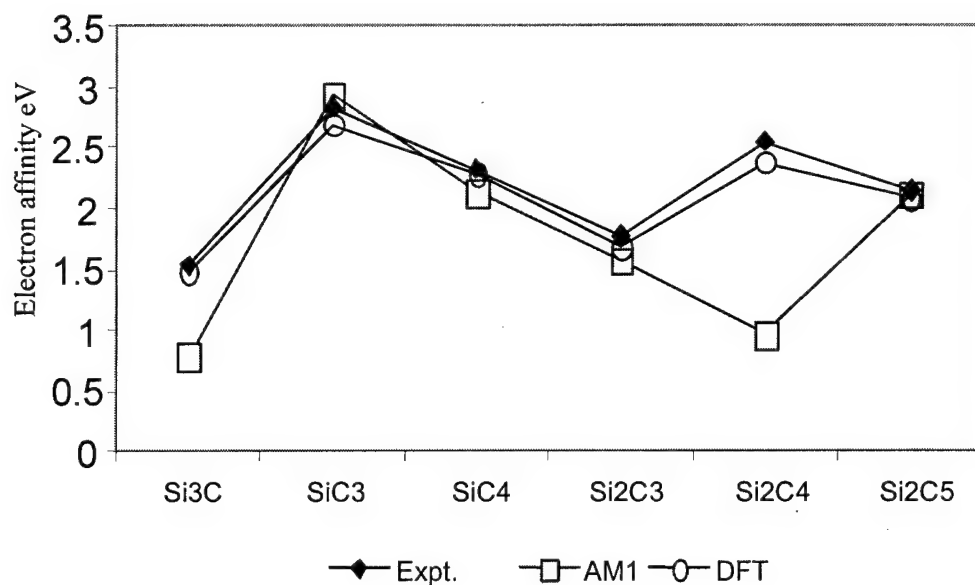
Figure 10. EA results calculated by AM1 and DFT method compared with experimental results for SiC clusters

For triplet state structure of Si_3C (shown in Figure 12), the C atom may be single bonded with the bottom two silicon atoms, and double bonded with the top silicon atom. This is unlikely because of the strained geometry and the tendency of silicon not to form double bonds. Alternatively, in the singlet three lone pairs may reside on three of the four atoms; either there is a pair of lone unbonded electrons with the top Si or on the carbon. In the triplet, there is a non-bonded single electron on both the center Si and C, which contribute to electron spin equal to 1. A more electropositive carbon favors the triplet electronic state. Because of predicting the wrong electronic state, AM1 gives incorrect result. The relative errors for AM1 and DFT methods are shown in Figure 11.
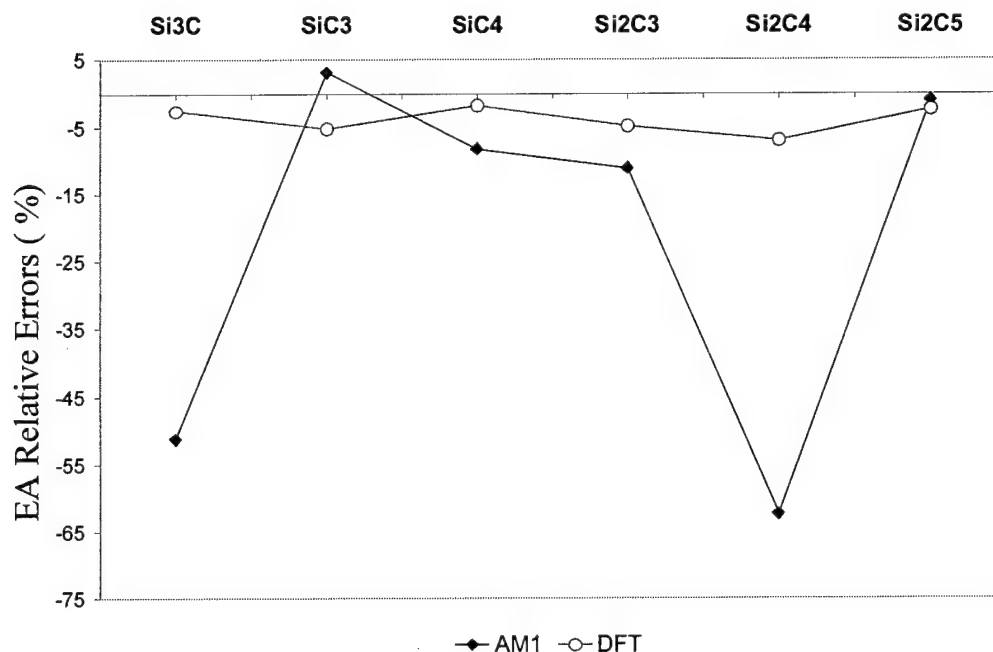
Figure 11. The EA calculation errors of AM1 and DFT method

From Figure 11, one can see that DFT method provides accurate and reliable results comparing to the experiment results. Since AM1 results oscillate, one can conclude that AM1 cannot give reliable results. The mean square root of errors in electron affinity calculation, DFT method has a negative offset 0.1 eV, ie, since DFT method gives stable results, one can use the mean square root of errors to correct other calculations that do not have experimental results to compare to.

Duan [14] has shown that for Si_2C_3 ROHF, B3LYP, MCSCF(20,20) and CAS(8,10) calculations all predict a similar centrosymmetric linear geometry as the ground S_0 state. In the T_0 state, the electronic correlation corrections in DFT or post SCF methods predict longer bond lengths for Si-C and C-C bonds than

does the HF method. In T_0, the Si-C bonds stretch about 0.06Å while the C-C

bond does not change, with respect to the values for the S_0 state. The cluster in

the T_0 state has a calculated energy about 0.9 - 1.9 eV higher than energy of the S_0

state depending on the calculation methods. The HF method gives lowest T_0

energy while the CAS (8,10) calculation produces the highest one. Correlation

corrected methods of B3LYP, MCSCF (20,20), and CAS(8,10) result in T_0

energies ranging from 1.4 eV to 1.9 eV. Increasing the quality of the basis set

seems to increase the singlet-triplet gap. The HF methods predict that carbons

adjacent to silicon atoms to be too electopositive, favoring the triplet state. HF

methods, including AM1, which have small basis sets do not accurately predict

relative energies of the singlet and triplet states.

IV. Study of Si_mC_n Clusters ($m \leq 4, n \leq 4$) Using DFT Method

For this study, all DFT calculations were performed on a Sgi O2 workstation with IRX 6.5 operation system IRX 6.4, using the software package "Jaguar" 4.0. The restricted open shell calculation method (RODFT) was used throughout the calculations.

4.1 Study the Ground State Structures of Small SiC Clusters

Ground state means the lowest energy electronic state. Structure means the arrangement between different atoms in molecules, and the distances between those atoms. To find the ground state structure for each molecule is the most essential task for molecular modeling. In this work, ground state structures are obtained by predicting optimized structures with minimum singlet and triplet energies.

4.1.1. Mapping the Ground State Structures. Sixteen ground state structures are found using DFT: B3LYP functional and cc-pVDZ //cc-pVDZ(-D) calculations. They are listed in Figure 12.
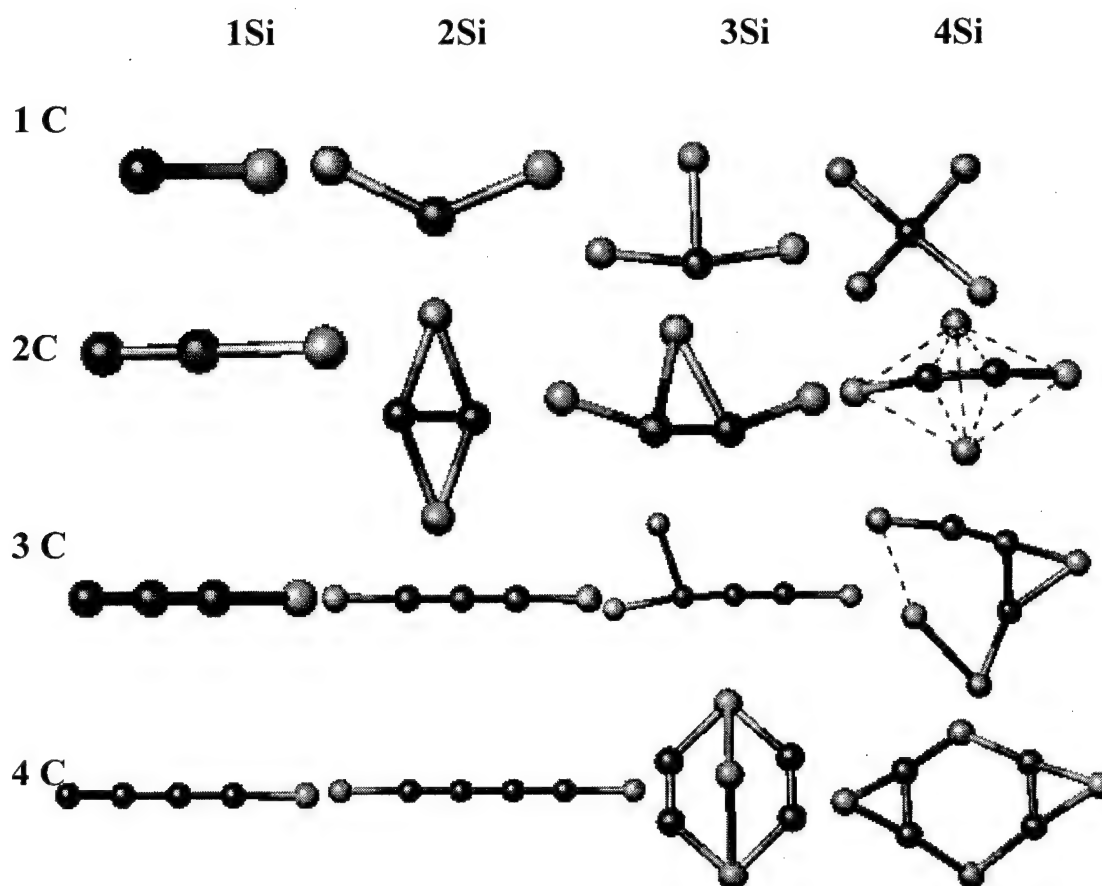
Figure 12. The ground state structure of Si_mC_n clusters predicted by DFT method

For linear structures in Figure 12, one concludes that clusters with even total number of atoms tend to have the triplet ground state structure. The linear clusters with odd total number of atoms tend to have the singlet ground state structure. All bent structures are singlet ground states. As the silicon atom number increases to 3 or above, no linear ground state structure is founded. In this $m \times n = 4 \times 4$ system, we see that the mixed silicon carbide clusters tend to show characteristics like pure silicon cluster when the silicon atom increases to 3 or more. These structures tend to be nonlinear and three-dimensional. When the

number of carbon atoms is much larger than the number of silicon atoms in the mixed cluster, the cluster tends to show the characteristic of pure carbon. These clusters tend to have linear structures.

4.1.2. Difference in structure between the singlet, triplet and doublet states.

In AM1 calculations, there is little change between singlet and triplet structures. But in DFT calculations, some of the structures are significantly changed. The Si-C bonds in triplet states tend to have a longer bond length and the structure tends to expand relative to structures found in the singlet ground state. The doublet state bond lengths are between singlet state and triplet state values, but closer to the singlet state. For instance, these clusters and their structures are shown in the Figure 13.

S_0 -944.601121	-944.575858	-944.649768
S_0 -982.668917	-982.651510	-982.746645
S_0 -1020.728641	-1020.559614	-1020.788808
S_0 -1196.021594	-1195.930076	-1196.101824
S_0 -1310.233110	-1310.2045553	-1310.308155
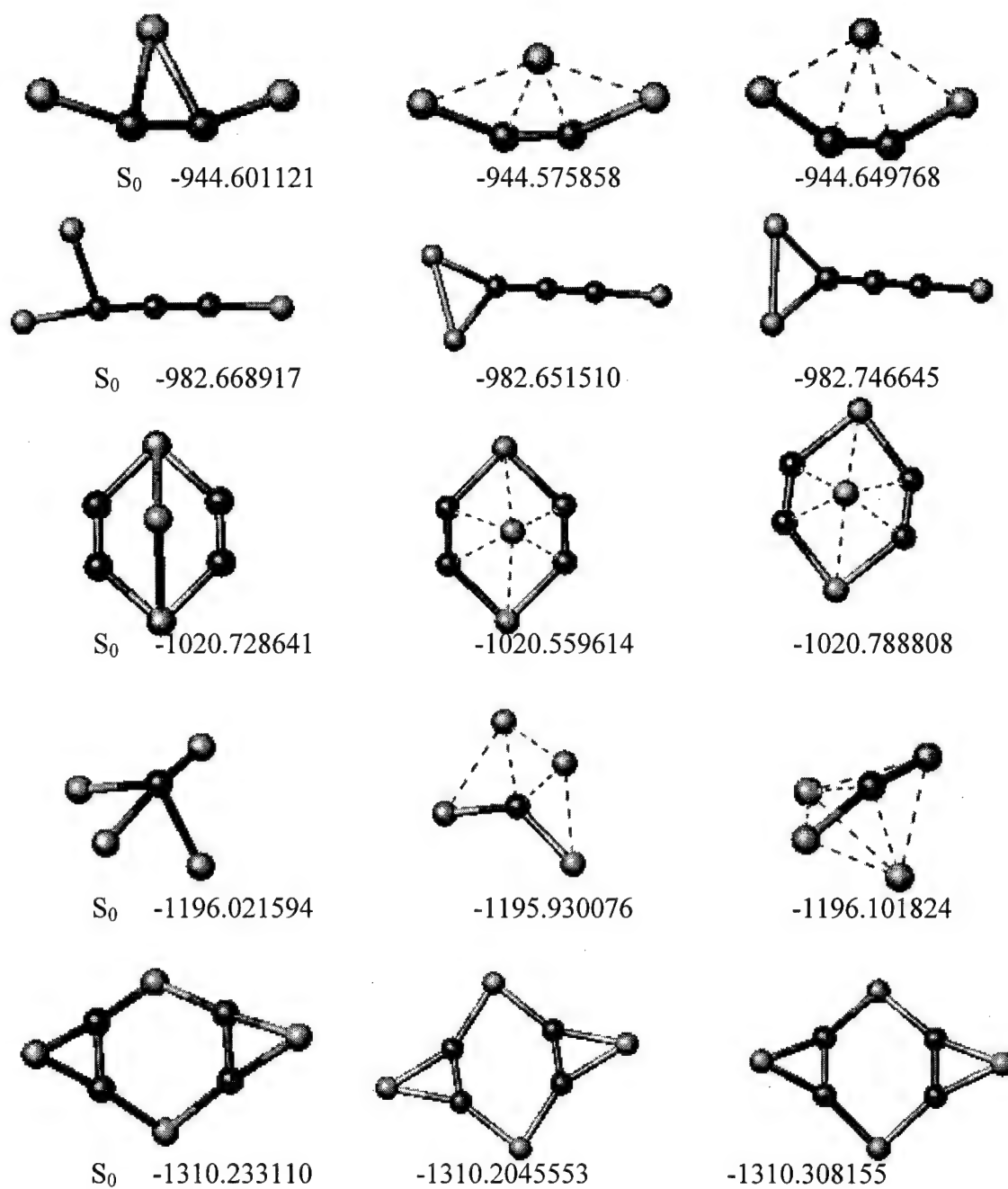
Figure 13. The geometry change with different electronic state (singlet, triplet, doublet state) for certain clusters

65

The dots between two atoms show that the bond lengths are longer than usual bond lengths. For C_2Si_3, C_4Si_3 and C_1Si_4 clusters, triplet state and doublet states have longer Si-C bond lengths than the singlet states. The Si-Si bond lengths are the opposite, for C_2Si_3, C_3Si_3 and C_1Si_4 clusters, the Si-Si bond lengths are shorter than for the singlet state structures. . These clusters in Figure 13 have three characters in common.

1) They are rich-silicon clusters;

2) They have bent structures;

3) They have singlet ground state structures.

The explanations follow.

When carbon and silicon atoms form the chemical bonds, carbon atom is very flexible. Carbon atoms favor sp, sp^2, and sp^3 hybridization. On the other hand, silicon atoms only favor sp^3 hybridization. For the rich silicon clusters, the silicon atoms are dominant, ie, the sp^3 hybridizations are dominant, and therefore, they have bent structures. In addition, silicon atoms that we can observe from Figure 12 and Figure 13 tend to be at the terminal positions of molecules where it is able form a double bond or to form a pair of lone electrons that is proven to form stable in silicon electronic structures. This pair of lone electron will contribute to the zero multiplicity spin in the molecules, so we see singlet ground states. In singlet state, silicon rich molecules form strained multiple single chemical bonds to achieve the stable structures, so we see these singlet state structures tend to be more compact than triplet structures.

4.2 Calculate the Electron Affinity (EA)

Dr. Lineberger's group used photo-electron-spectroscopy (PES) to detect some silicon carbide clusters produced by cathodic discharge. The experiment results are listed in the Table 3. The principle of PES uses Einstein's photoelectron effect formula:

$$E_b = E_{photon} - E_{kinetic} - \Phi \qquad (4\text{-}1)$$

where E_b is the core-electron binding energy, E_{photon} is the excited photon energy, $E_{kinetic}$ is the kinetic energy of electron in vacuum which can be detect, Φ is the spectrometer work function, which is a constant for a given analyzer. In this process a photon interacts with an atom or molecule liberating an electron. From this process, a lot of properties of materials are revealed. For example, the lowest electron binding energy is the electron affinity (EA). Dr. Lineberger's group has observed and analyzed several silicon carbide clusters' ground state PES spectra, and measured the electron affinities and vibration frequencies. We compare calculation results to Dr. Lineberger's experimental results, to determine the accuracy and reliability of the calculations.

It is a very difficult task to accurately calculate the electron affinity by quantum mechanical method. The principle is to use the formula:

$$E_{EA} = E_0 - E_{anion} \qquad (4\text{-}2)$$

Where E_{EA} is the energy of electron affinity (EA), E_0 is the ground state energy, and E_{anion} is the ground state the energy of anion. The ground state energy can be calculated by optimizing the minimum energy of ground singlet or triplet state.

Here, singlet means the valence electrons of this molecule has multiplicity of one and zero charge; triplet means the valence electrons of this molecule has multiplicity of three and zero charge; the anion energy, ie., doublet energy, where doublet means the valence electrons of this molecule has multiplicity of two and with "-1" electron charge. The calculation accuracy of electron affinity is not only dependent on the accuracy of the calculation of both the ground state (singlet or triplet) energy and the doublet energy. According to the variational principle (discussed in chapter two), with the increasing of basis sets, the calculation energy result should be more close to the exact energy. However, since the energy of both ground state and doublet state become more accurate as the number of basis functions increase, one cannot guarantee that the electron affinity result becomes more accurate. Because the electron affinity is the difference between ground state energy (singlet or triplet) and doublet state energy (anion), the subtraction of two energies may cancel out the improvement in energy with increasing basis set.

The electron affinity calculation results and the experimental results silicon carbide clusters are listed in Table 8. One can see that the DFT method predicts good agreement with experimental results. Also, DFT calculations provide results for clusters that were not observed by experiments.

Table 8. Electron affinity (EA) results in eV calculated by DFT:B3LYP/cc-pVDZ+ method for Si_mC_n clusters

n \ m	1 Si	2 Si	3 Si	4Si
1 C	2.259 T_0	0.930 S_0	1.491 S_0 **1.535***	2.312 S_0
2 C	1.665 S_0	1.383 S_0	1.539 S_0	0.964 S_0
3 C	2.692 T_0 **2.845***	1.684 S_0 **1.769***	2.296 S_0	1.869 S_0
4 C	2.285 S_0 **2.327***	2.378 T_0 **2.556***	1.887 S_0	2.237 S_0
5 C		2.043 S_0 **2.136**		
6 C		2.689 T_0 **2.409**		

T_0 indicates the triplet state, S_0 indicates the singlet state.

Furthermore, using these calculations can help us to explain some phenomena encountered in experiments. For instance, Dr. Lineberger's group found during these experiments that they did not observe any rich-silicon clusters with silicon number more than 3. For the CSi_3 cluster, they are not able to see until it is cooled down in temperature. Use of DFT calculation results we can give an explanation illustrated in Figure 14.

$C_4Si_4 \xrightarrow{\text{Add energy 0.114 eV}} CSi_3 + C_3Si^-$

$C_4Si_4 \xrightarrow{\text{Add energy 1.675 eV}} CSi_3^- + C_3Si$

$C_3Si_3 \xrightarrow{\text{Add energy 1.729 eV}} CSi_2 + C_3Si^-$

$C_3Si_3 \xrightarrow{\text{Add energy 2.193 eV}} CSi_2^- + C_2Si$
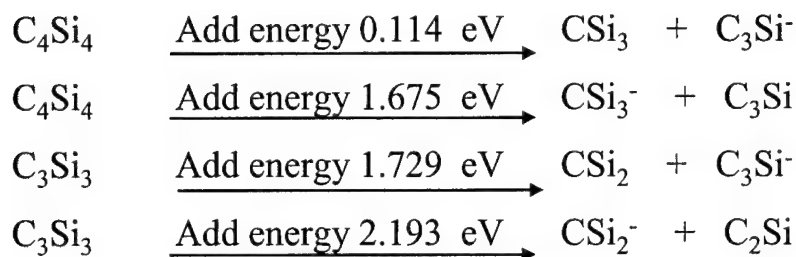
❖ Need more energy to create rich-Si anion than create rich-C anion.

CSi_5 has electron affinity $=1.270$ eV

C_5Si has electron affinity $=3.091$ eV

❖ Rich-C anion is more stable than the rich-Si anion.

Figure 14. The stability of silicon-rich clusters and their anions

From Figure 14, one can conclude that silicon-rich cluster anions are hard to make and difficult to keep. This may be the reason that Dr. Lineberger's group did not see rich silicon clusters in PES. In order to see rich silicon clusters, we predict that they need to observe rich silicon cluster in neutral state instead of anion state.

4.3 Evaluation of Accuracy and Reliability of DFT Calculations

In this work, the purpose is to find the quantum mechanical calculation method that can accurately model the small SiC clusters. In order to evaluate the accuracy of calculations, we compare the calculation results with experimental

results. The comparison of DFT results with the experimental results is listed in

Table 9.

Table 9. A comparison of DFT calculation results with experimental results

Cluster		Si_3C	SiC_3	SiC_4	Si_2C_3	Si_2C_4	Si_2C_5	Si_2C_6
Experiment Structure		Rhombic	Linear	Linear	Linear	Linear	Linear	Linear
DFT Prediction		Rhombic S_0 Fig. 4-1	Linear T_0 Fig. 4-1	Linear S_0 Fig. 4-1	Linear S_0 Fig. 4-1	Linear T_0 Fig. 4-1	Linear S_0 Fig. 4-1	Linear T_0 Fig. 4-1
DFT Calculated EA (eV)		**1.491**	**2.692**	**2.285**	**1.684**	**2.378**	**2.087**	**2.689**
Calculated Frequency (cm^{-1})	f_1	326		571	466	759	36	2096
	f_2	499	2013	1182	904		381	
	f_3	1085		1895	1577	1657	2067	
Exp. EA (eV)		**1.535**	**2.839**	**2.327**	**1.769**	**2.556**	**2.136**	**2.409****
Exp. Frequency (cm^{-1})	f_1	315	1950	565	420	845	40	3735**
	f_2	490	2015	1105	910	1175	340	
	f_3	12575**	2185	1860	1485	1860	8105	
EA Error		-0.044	-0.147	-0.042	-0.085	-0.178		
Error of f_1 cm^{-1}		11		6	46	-86	-4	
Error of f_2 cm^{-1}		9	-2	77	6		41	
Error of f_3 cm^{-1}				35	92	-203		

*Calculation method: DFT: 3BLYP/ccpvDZ+//cc-pVDZ
**Experimental result might have an error

Table 9 shows that all the results predicted by DFT method are in good

agreement with experimental results. The average error of electron affinity

calculations is less than -5% using medium size of basis set (DFT: B3K/cc-

pVDZ+). The largest absolute error of electron affinity calculation is for the C$_4$Si$_2$ cluster, which is -0.178 eV. The mean square root of error is -0.1 eV, which is close to the largest absolute error, so we can use the mean square error offset to correct those EA calculation results that they do not have the experiment to compare to. For vibration modes, the calculation vibration frequency results have an average mean square root error of -72.5 cm^{-1} wave numbers.

4.3.1. The Geometry Change Respecting Different Size of Basis Sets.

The geometry optimization is sensitive to the size of the basis sets, but less sensitive than the energy. Basically, the accuracy increases with the size of the basis sets. However, the geometry optimization is very time consuming. For example, a single geometry optimization for Si$_2$C$_4$ cluster takes 5 hours using basis set cc-pVDZ (-d), takes 10 hours using basis set cc-pVDZ, and takes 500 hours using basis set cc-pVTZ+. In order to save the computing time and still accurately model clusters, the common technique is to optimize molecule structures at the lower basis set level, such as cc-pVDZ(-d). Then optimize those structures having lowest energy using larger basis sets. Using this technique, we get the ground state structures that are listed in the Figure 12. We choose cc-pVDZ(-d) basis sets for first geometry optimization, and optimize those structures with relatively low energy using cc-pVDZ basis set. It is needed to know if there any difference with geometry if we choose much larger basis sets to optimize them, for instance using cc-pVTZ+ instead of using cc-pVDZ.

The geometry change of clusters respecting the different size of basis sets is studied on two molecules. The selection is base on two reasons. First, these two clusters have been observed and detected by Dr. Lineberger's group, so we have the experimental results to compare with the calculation results. Second, C_4Si_2 represents the linear structure cluster and rich-carbon cluster, while Si_3C represents bent structure cluster and rich-silicon cluster. Here we use letter A to represents the optimized structure which is calculated at the condition of choosing basis set cc-pVDZ (medium size); letter B represents the optimized structure that is calculated at the condition of using basis set cc-pVTZ+ (larger sized basis set), shown in Figure 15. A and B structures are similar. A detailed comparison of bond length and bond angle is listed in the Table 10. The computer time for getting structure A is about 10 hours on Sgi O2 workstation. For structure B, the same calculation requires more than 500 hours.

Si_2C_4
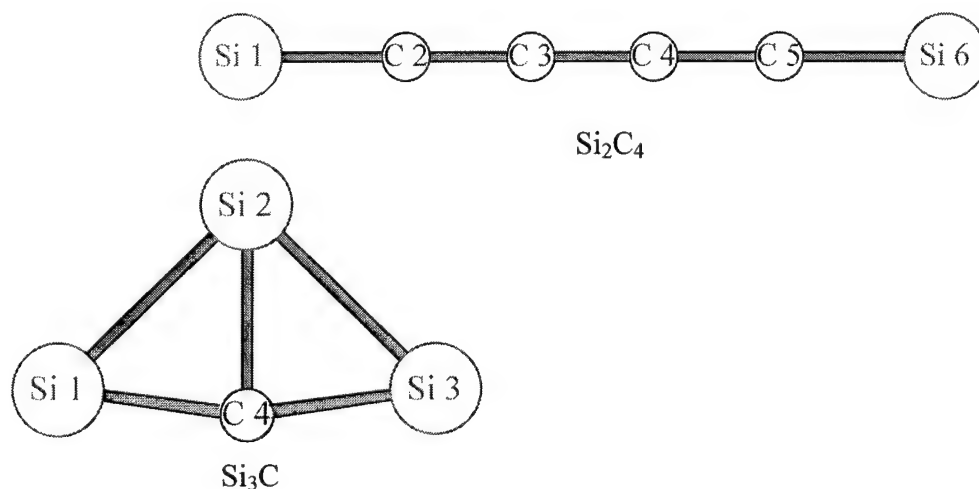
Si_3C

Figure 15. The clusters used to study the geometry change using different basis sets

Table 10. A comparison of examples of geometry changes

with different basis sets

	Si_3C					
Structure	A *		B **		Differences Between A & B	
State	S_0	D_0	S_0	D_0	S_0	D_0
No. Basis Functions	68 Bond Length (Å)		220 Bond Length (Å)		Bond Length (Å)	
Si_1-C_4	1.778	1.805	1.762	1.789	-0.016	-0.016
Si_2-C_4	1.967	1.930	1.944	1.913	-0.023	-0.017
Si_3-C_4	1.778	1.805	1.778	1.805	0	0
Si_1-Si_2	2.471	2.445	2.446	2.421	-0.025	-0.024
Si_2-Si_3	2.471	2.444	2.471	2.445	0	0.001
Bond Angle (°) Si_1-C_4-Si_2	82.413	81.684	82.400	81.600	-0.013	-0.084
	Si_2C_4					
Structure	A *		B **		Differences Between A & B	
State	T_0	D_0	T_0	D_0	T_0	D_0
No. of Basis Functions	92 Bond Length (Å)		320 Bond Length (Å)		Bond Length (Å)	
Si_1-C_2	1.738	1.713	1.725	1.702	-0.013	-0.011
C_2-C_3	1.282	1.283	1.271	1.298	-0.011	0.015
C_3-C_4	1.301	1.309	1.293	1.275	-0.008	-0.034
C_4-C_5	1.282	1.283	1.271	1.298	-0.011	0.015
C_5-Si_6	1.738	1.713	1.725	1.702	-0.013	-0.011

*   A is the structure optimized using basis set cc-pVDZ.
** B is the structure optimized using basis set cc-pVTZ+ .
S_0 - singlet state, T_0 - triplet state, D_0 - doublet state

From Table 10, one can conclude that the changes in geometry with basis set size are small. For cluster Si_3C, the average bond length changed 0.013 Å, the average bond angle changed 0.048 ° when the basis set function increase about 3 times from 68 to 220, and the CPU time increased from 5 hours to 500 hours. For cluster C_4Si_2, the average bond length changed 0.014 Å, and there was no bond angle change, when the number of basis set functions increase from 92 to 320,

more than 3 times larger.

At this point, it can be easily concluded that the geometry will not change or only have a very small change after the basis set is increased to a certain level. Knowing this can save us a lot of work and CPU time. In SiC system, cc-pVDZ seems a good stopping point for geometry optimizing. However, one may wonder that small change in geometry may cause a tremendous change in electronic properties. Therefore, comparison of single point calculations for energy is necessary for structures A and B.

4.3.2. The electron affinity change for SiC clusters using different size of basis sets.

We learned in the above section that the geometry changes between structure A and B are very small in SiC clusters. Structure A is the structure optimized at the basis sets of cc-pVDZ (lower basis sets), structure B is the structure optimized at the basis set of cc-pVTZ+ (higher basis sets). One wants to know if these small geometry changes lead to large changes in electronic properties of SiC clusters. The single point calculations are performed using various basis sets, where single point calculation means calculating the molecule's energy using different basis sets at frozen structures A and B (no geometry optimization). The result of energies and electron affinities are listed in Table 11. Observing the comparisons between A and B, the difference of electron affinity between structure A and structure B are zero or 0.001 eV, which means that there is no change or very small change between structure A and structure B in electron affinity results.

Table 11. The electron affinity comparison between structure A and B

Cluster	CSi_3						
Basis Set	A* Energy (eV)		B** Energy (eV)		EA result (eV)		$EA_A - EA_B$
	S_0	D_0	S_0	D_0	A (eV)	B	(eV)
cc-pVDZ+	0.000	0.000	0.000	0.000	1.491	1.491	0
cc-pVTZ	-1.082	-0.947	-1.109	-0.972	1.355	1.355	0
cc-pVTZ+	-1.109	-1.082	-1.136	-1.108	1.464	1.463	0.001
Experimental Result (eV)	1.535						
Cluster	C_4Si_2						
Basis Set	A* Energy (eV)		B** Energy (eV)		EA result (eV)		$EA_A - EA_B$
	T_0	D_0	T_0	D_0	A	B	(eV)
cc-pVDZ+	0.000	0.000	0.000	0.000	2.378	2.358	0.020
cc-pVTZ	-1.615	-1.502	-1.588	-1.497	2.265	2.267	-0.002
cc-pVTZ+	-1.636	-1.613	-1.639	-1.628	2.354	2.356	0.002
Experimental Result (eV)	2.556						

*A is the structure optimized using DFT: B3LYP/cc-pVDZ;
**B is the structure optimized using DFT: B3LYP/cc-pVTZ+//cc-pVDZ
S_0 indicate the singlet state, T_0 indicate the triplet state, D_0 indicate the doublet state

4.4 The Electron Affinity Results Versus Basis Sets

The choice of basis set directly effect on the choice of trial wave function, so it effect on the accuracy of calculation results. A comparison of electron affinity results and their accuracy respect to the selection of basis sets are listed in Table 12.

Table 12. A comparison of electron affinity calculation accuracy versus the size of basis set

Cluster	Si_3C	SiC_3	SiC_4	Si_2C_3	Si_2C_4	Si_2C_5	Si_2C_6
cc-pVDZ No. basis function	68	60	74	78	92	106	120
EA Results (eV)	**1.289**	**2.392**	**2.000**	**1.470**	**2.192**	**1.932**	**2.522**
cc-pVDZ+ No. basis function	104	96	119	123	146	169	192
Results (eV)	**1.491**	**2.692**	**2.285**	**1.684**	**2.378**	**2.087**	**2.689**
cc-pVTZ No. basis function	144	136	169	173	206	239	272
EA Results (eV)	**1.355**	**2.564**	**2.134**	**1.532**	**2.265**	**1.962**	**2.600**
cc-pVTZ+ No. basis function	220	212	264	268	320	372	424
EA Results (eV)	**1.464**	**2.694**	**2.265**	**1.652**	**2.354**	**2.043**	**2.668**
Experiment EA result	**1.535**	**2.839**	**2.327**	**1.769**	**2.556**	**2.136**	**2.409****
Errors using cc-pVDZ	0.245	0.447	0.327	0.299	0.365	0.204	
Errors using -pVDZ+	0.044	0.147	0.042	0.085	0.178	0.049	
Errors using cc-pVTZ	0.18	0.275	0.193	0.237	0.291	0.174	
Errors using cc-pVTZ+	0.071	0.145	0.062	0.117	0.202	0.093	

*Calculation method: DFT: 3BLYP

**This might indicate an error in experiment.

The electron affinity results in Table 12 are plotted in Figure 16.
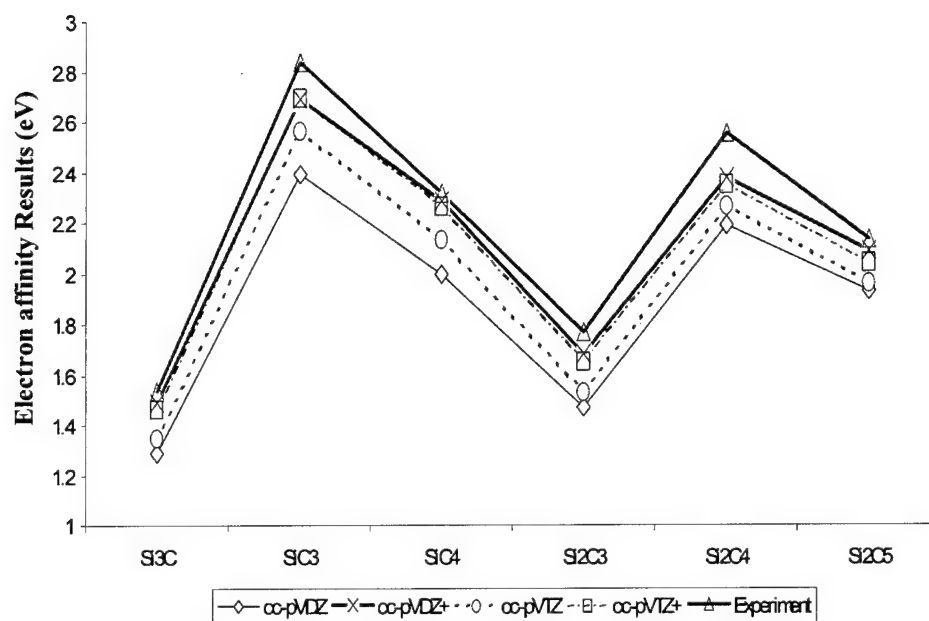
Figure 16. The relationship of calculation accuracy with choice of basis sets

Something unusual appeared in Table 12 and Figure 16. According to variational principle, with increasing basis set, one should get better energy results. Here we found that during single point calculation, the value of EA error is on the order of: cc-pVDZ > cc-pVTZ > cc-PVTZ+ > cc-PVDZ+. Taking Si_3C cluster as an example, the number of basis function is in the order of 68, 144, 220, 104. The number of basis function of cc-pVDZ+ is less than the number of basis functions of cc-pVTZ and cc-pVTZ+, but the electron affinity result using cc-pVDZ+ is more accurate than the result using cc-pVTZ and cc-pVTZ+. Why? It is obvious that adding diffuse function to the basis sets significantly improved the electron affinity accuracy from basis sets cc-pVDZ to cc-pVDZ+. However, comparing the basis set both having diffuse functions, cc-pVDZ+ and cc-pVTZ+,

even though their electron affinity results are very close to each other and to the experimental results, why does cc-pVDZ+ basis sets give more accurate electron affinity results than using basis sets cc-pVTZ+?

Recall from section 4.2 the definition of electron affinity is the energy difference of doublet state and the ground state singlet (triplet) state. From chapter two we know that the energy calculated using ab initio method or DFT method is an approximate energy, which improves with basis set improvements, according to variational principle. The more basis functions one uses, the lower energy one gets, and the more accurate results. In order to look closely to see how the energy improved respecting to the difference size of basis set, a detailed calculation energy results are in Table 13.

Observing Table 13, one can see that the energies are decreasing with increasing basis set, which is consistent with variational principle. However, the energy-decreasing rate is different with respect to the differences in basis sets. The ground state energies (singlet, or triplet state) decrease faster than the anion energies (doublet state) when the size of basis functions is enlarged without adding diffuse functions. On the other hand, anion energy decreases faster than the ground state energy when only adding diffuse functions to the basis sets. These cause a nonlinear relationship between electron affinity calculation results with the changes in basis sets. Therefore, one cannot expect to always get more accurate electron affinity results by simply increasing basis sets.

Table 13. A comparison of basis set effect on the energy change

Cluster	DFT:3BLYP/cc-pVDZ Energy result (a.u.)		DFT:3BLYP/cc-pVDZ+ Energy result (a.u.)		Energy Decrease (a.u.)	
	E_0 *	ED **	E_0 *	ED **	E_0 *	ED **
CSi$_3$	-906.53394	-906.58148	-906.53778	-906.59275	0.00384	0.01128
SiC$_3$	-403.58992	-403.67816	-403.59565	-403.69496	0.00573	0.01680
SiC$_4$	-441.70644	-441.78005	-441.71286	-441.79713	0.00642	0.01707
Si$_2$C$_3$	-693.18082	-693.23505	-693.18548	-693.24760	0.00466	0.01255
C$_4$Si$_2$	-731.23908	-731.31990	-731.24544	-731.33314	0.00636	0.01324
Si$_2$C$_5$	-769.34107	-769.41233	-769.34821	-769.42517	0.007147	0.01285
Si$_2$C$_6$	-807.40428	-807.49734	-807.41143	-807.51061	0.007154	0.01327
Cluster	cc-pVDZ+ Energy result (a.u.)		cc-pVTZ+ Energy result (a.u.)		Energy Decrease (a.u.)	
	E_0	ED	E_0	ED	E_0	ED
CSi$_3$	-906.53778	-906.59275	-906.57864	-906.63264	0.04086	0.03988
SiC$_3$	-403.59565	-403.69496	-403.63294	-403.73229	0.03729	0.03734
SiC$_4$	-441.71286	-441.79713	-441.76163	-441.84515	0.04877	0.04803
Si$_2$C$_3$	-693.18548	-693.24760	-693.23670	-693.29765	0.05122	0.05004
C$_4$Si$_2$	-731.24544	-731.33314	-731.30573	-731.39257	0.06029	0.05943
Si$_2$C$_5$	-769.34821	-769.42517	-769.42001	-769.49537	0.07180	0.07020
Si$_2$C$_6$	-807.41143	-807.51061	-807.49283	-807.59123	0.08139	0.08062

* E_0 indicates the ground state energy; ** ED indicates the doublet state energy

The energy change with respect to enlarging the basis sets and adding diffuse function to basis sets, ie., basis set change from cc-pVDZ+ to cc-pVTZ+ , is plotted in the Figure 17.
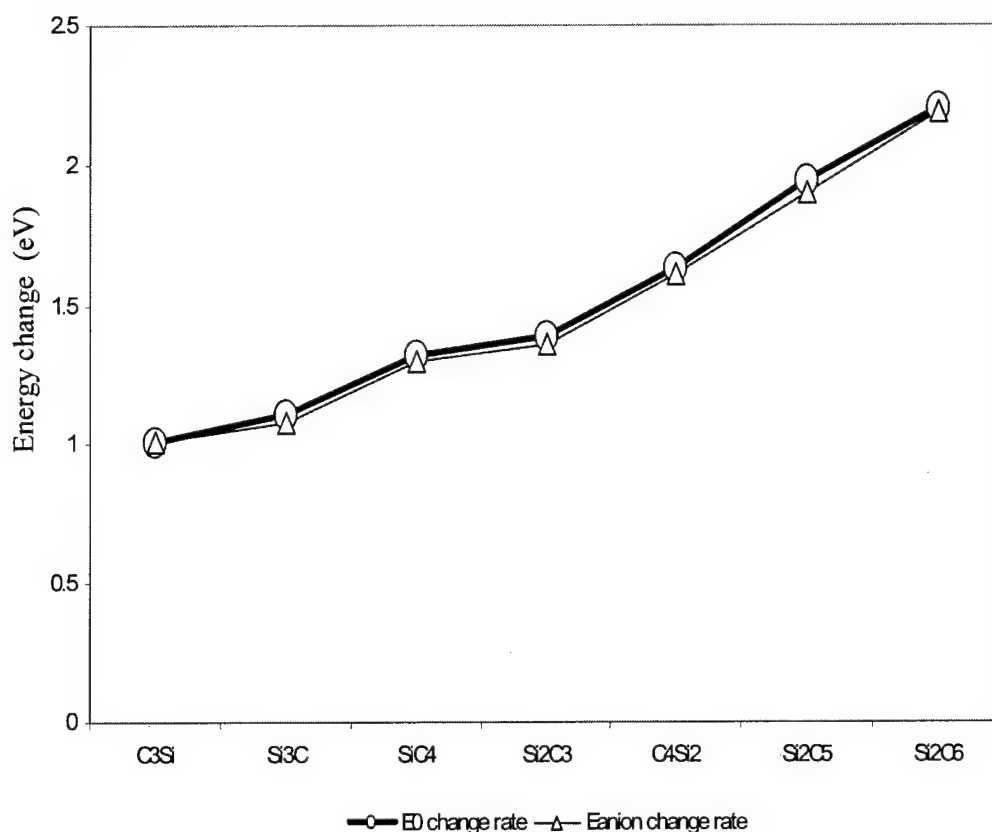
Figure 17. The energy change with change of basis sets (from cc-pVDZ+ to cc-pVTZ+) for SiC clusters

E_0 indicates the ground state energy (singlet or triplet state);
E_{anion} indicates the doublet state energy

One can see from Figure 18 that, the rate of energy change between ground state and the doublet state is very small using basis set cc-pVDZ+ to cc-pVTZ+. This is the reason we see in Figure 17 that the electron affinity result using cc-pVDZ+ and cc-pVTZ+ are very close. Figure 18 shows enlarging the basis set by adding diffuse function into both basis sets, the ground state (singlet or triplet state) energy decrease is a little faster than the energy decrease of anion (doublet

state). One can see that increasing basis set size without adding diffuse functions improved mainly the ground state energy. On the other hand, only adding diffuse function to basis sets improves mainly the doublet energy (anion energy). For same basis set, adding only diffuse function, the energy of the anion (doublet state) decreases at a much greater rate than the ground state (singlet or triplet state). The different rate of energy change results in a nonlinear change of the electron affinity with increasing basis set size. The relationship of energy reducing rate versus adding diffuse functions to basis sets from cc-pVDZ to cc-pVDZ+ are plotted in the Figure 18.
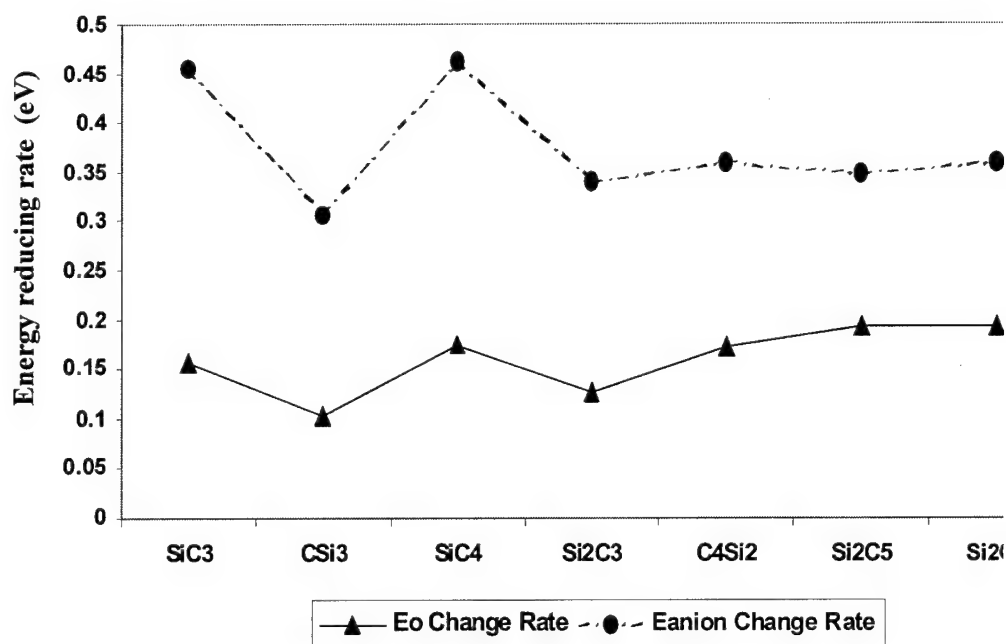
Figure 18. The energy reducing rates respecting to adding diffuse functions to basis sets

E_0 indicate the ground state energy, E_{anion} indicate the doublet state energy

Again, take Si_3C cluster as an example. From Table 13, Figure 17 and Figure 18, one can see that the value of energies is become lower with increasing the size of basis functions, which is consistent with the variational principle.

Increasing the basis set size without adding diffuse function, improves mainly the ground state energy, so the electron affinity result accuracy is improved by more than 4.0% with increasing basis set cc-pVDZ to cc-pVTZ. Adding diffuse functions to the basis sets, the energy of doublet state is significantly improved. The accuracy of electron calculation is improved more than 13% by choosing cc-pVDZ+ instead of cc-pVDZ+. Therefore, when adding diffuse functions and enlarge basis set at same time, the accuracy of electron affinity might not be improved. The improved energy may be canceled by the subtraction.

In summary, adding diffusing function to the basis set is very important for SiC systems, it dramatically increases the accuracy of electron affinity result. Because silicon is a big atom with 3s, 3p electrons in its valence shell, the valence shell electrons are very different from electrons in the hydrogen atom. Therefore it requires more contraction functions, adding polarized functions or adding diffuse functions in the basis function to correct hydrogen like approximation.

4.5 The Time Scale of DFT Calculation

DFT calculation is cheaper than the post HF ab initio calculations (stated in chapter one & two). But no one knows exactly what is the time scaling of DFT

calculations for the SiC system. For our practical application, the time scaling is important. The CPU time that we discuss here are classified to two types of CPU time. First is the average CPU time per SCF iteration. Technically this is the only accurate way to scale the computational time. However, the total CPU time on a particular computer is important too, so we discusses the CPU time scaling of DFT calculation with the average CPU time and the total CPU time separately.

4.5.1. The Average CPU Time Per SCF Iteration. The relationship of CPU time (per SCF iteration) versus size of basis sets is plotted in Figure 19.
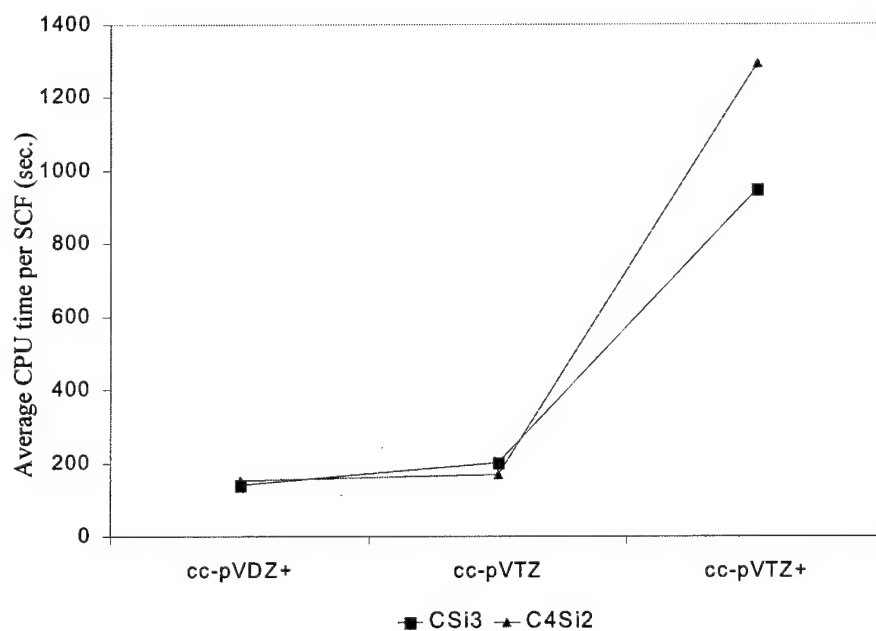
Figure 19. The average CPU time (per SCF iteration) versus basis sets

From Figure 19, one can see how the CPU time increases with the size of basis set. With mathematical fitting, one can conclude that the average CPU time

per SCF iteration of DFT calculation in SiC system approximately exponentially increases with the system size (the number of basis functions). For different basis sets, the exponential power is increase with the size of basis sets.

4.5.2. The total CPU time. The total CPU time used in single point calculations for SiC clusters are recorded in Table 14

Table 14. The relationship of total CPU time versus the size of basis sets

Cluster	Si_3C	SiC_3	SiC_4	Si_2C_3	Si_2C_4	Si_2C_5	Si_2C_6
No. basis functions cc-pVDZ+	104	96	119	123	146	169	192
Total CPU time (sec.)	2549	815	2185	2066	3472	5765	10849
No. basis functions cc-pVTZ	144	136	169	173	206	239	272
Total CPU time (sec.)	1961	1160	1517	740	948	3247	5249
No basis functions cc-pVTZ+	220	212	264	268	320	372	424
Total CPU time (sec.)	7447	4734	8193	4242	5736	18147	28708

From Table 14, one can see that the total CPU time has the order of: cc-pVTZ < cc-pVDZ+ < cc-pVTZ+. It may looks strange that the number of basis function of cc-pVDZ+ (104) is smaller than the number of basis function of cc-pVTZ (144), but the total CPU time of cc-pVDZ+ calculation is longer than the calculation time of cc-pVTZ.

4.5.3. The Total CPU Time vs. Adding Carbon Atom to System. To see

the increase in CPU time to add a carbon atom, a time scaling relationship for

adding carbon atoms to the cluster is shown in Figure 20 (Appendix E lists data).
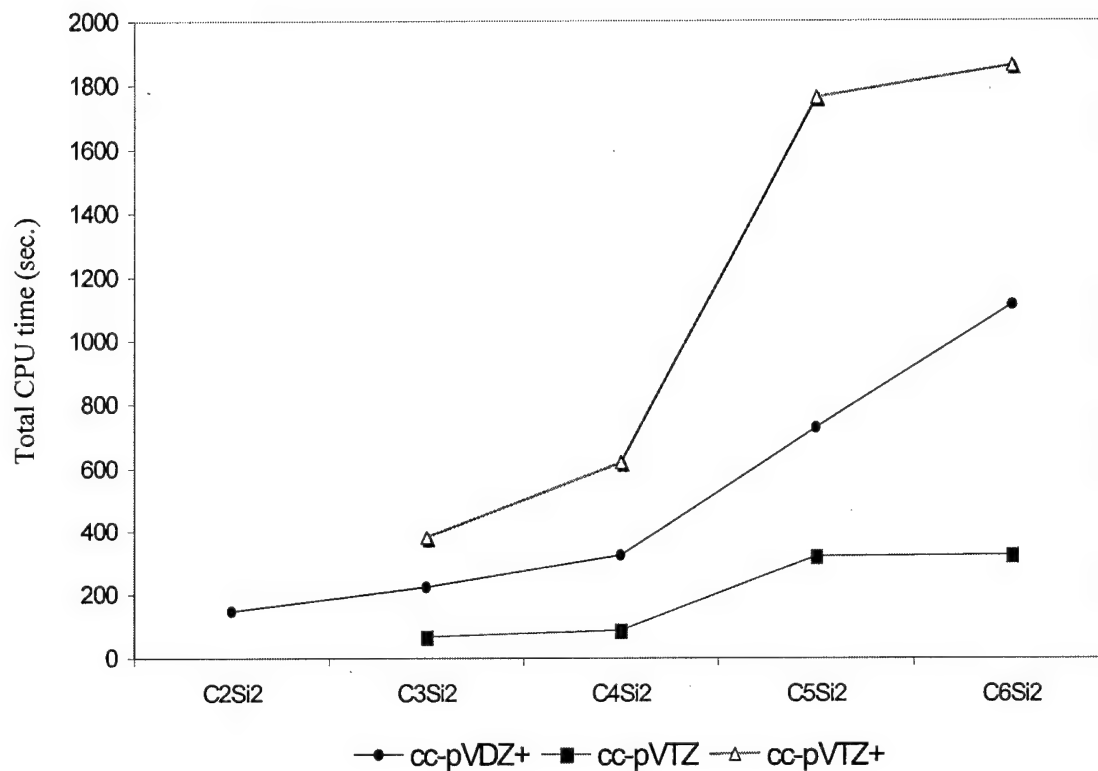
Figure 20. The total CPU time versus increasing C atoms in SiC system

For smaller size of basis sets, cc-pVDZ+ and cc-pVTZ, the total CPU time

looks almost a linear relationship for the SiC system with increasing number of

carbon atoms. The order of total CPU time is: cc-pVYZ+ > cc-pVDZ+ > cc-

pVTZ. Good fitting is found from Figure 20 for basis set cc-pVTZ+. The total

CPU time increases exponentially to the order of 1.6 th power with increasing C

atoms in the SiC system.

4.5.4. The Total CPU Time Versus Adding Silicon atom to SiC system.

A study of adding Si atoms to SiC system is performed. A plot can be view

in Figure 21, detailed data can be found in the Appendix E.
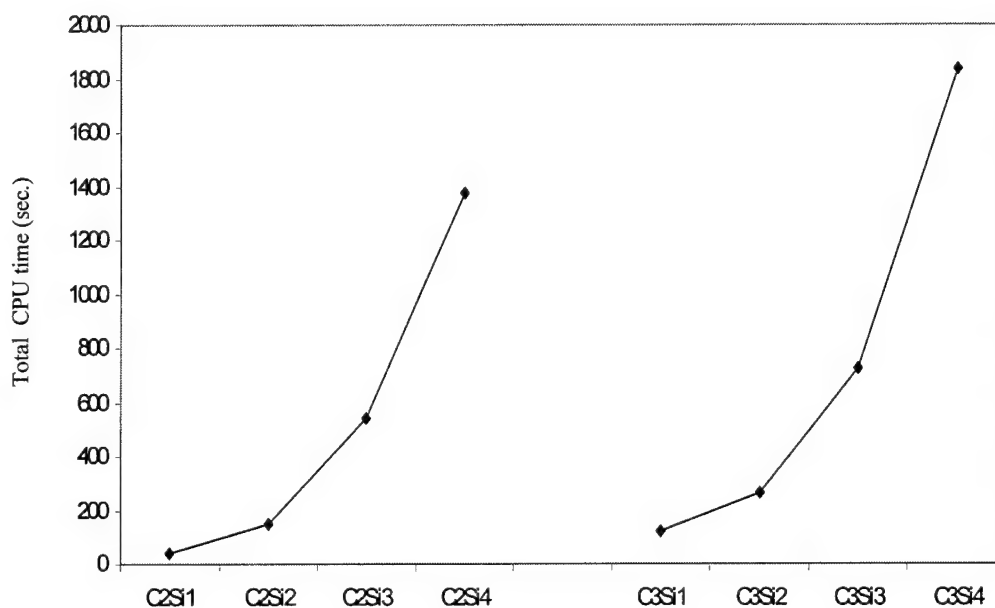
**Figure 21. The total CPU time versus increasing Si atoms in SiC clusters
using cc-pVDZ basis set**

Mathematical fitting of the DFT:B3LYP calculation times using cc-pVDZ+

basis set for SiC systems adding Si atoms shows that the total CPU time increases

with each silicon in the system on the order of the 2.2th power.

V. Conclusion

5.1 Problem Statement Review

Silicon carbide has a wide band gap. It is a very important semiconductor material for high temperature and high power applications. Many previous researches had been conducted on pure carbon and pure silicon clusters and solids. Only a few research studies had been done on mixed silicon carbide clusters. Surface chemistry of silicon carbide remains unknown. At present, there are no detailed theoretical or experimental models of silicon carbide surface chemistry. Using quantum mechanical method to model silicon carbide surface is an economic and efficient approach, which can help understanding of the surface chemistry at the atomic and molecular level, contributing to significant control of epitaxial silicon carbide film processes.

Surfaces are often modeled using molecular clusters, which are too small to accurately represent the mechanical environment of bulk materials. Shoemaker [4] successfully modeled the surface formation using a hybrid quantum mechanics and molecular mechanics (QM/MM) method. He used ab initio methods to calculate optimized structures of small clusters, and then embedded these clusters in a large system using molecular mechanics method to calculate the large system. This model combines the accurate ab initio method and the efficient molecular mechanics method; which minimize the computation time consuming while maintaining the effect of the bulk constraint.

The key to modeling surface chemistry is to find an accurate ab initio method that can be used to accurately model the small cluster. To judge the accuracy of ab initio calculations one compares the calculation results with the experimental results. The scope of this work is to find the quantum mechanical method that can accurately model small silicon carbide clusters, and prepare to model the surface chemistry and defect structures of silicon carbide bulk materials in the future.

Dr. Lineberger's group provides experimental results using photoelectron spectroscopy (PES). These results include the overall structure, the electron affinity, and the vibration frequencies of observed clusters (see reference [15]).

Previous research shows that a DFT method predicts more accurate electron affinity results than very high level ab initio methods, such as CAS (8,10) and MCSCF (20,20) [14]. So, a DFT method is employed in this work for modeling Si_mC_n cluster molecules. A comparison of experimental results with calculations is shows the accuracy and the reliability of DFT calculations. The factors that affect the accuracy of DFT calculations, such as the size of basis set and properties of the basis set, are discussed. From a practical point of view, the time scaling of DFT method for SiC system is also discussed.

Semi-empirical method, AM1 is also briefly discussed. It focused on the accuracy of AM1 calculations.

5.2 Results Review and Conclusions

5.2.1. Ground State Structures Predicted by DFT Method. Sixteen

ground state structures of Si_mC_n clusters ($m \times n = 4 \times 4$), found using DFT:

B3LYP calculation, have following properties:

1) The clusters tend to have linear structures when the number of carbon

   atoms is larger than the number of the silicon atoms. Only one exception

   is C_4Si_3 cluster. For C_4Si_3, it has a 6-member ring structure (see Figure 4-

   1), all C atoms have double bonds, Si atoms are at the end of molecule.

   The top Si atom share 2 electrons with two Si atoms in the 6-member ring,

   and other two electrons form an pair of lone electrons which is proven to

   be a stable structure. This bonding is very similar to the bonding of C_4Si_2

   cluster.

2) SiC molecules tends to have maximum C-C bonds, because C-C bond are

   very strong bonds; SiC molecules tend to have minimum Si-Si bonds,

   because Si-Si bond are weak. The Si atoms go to terminal positions of

   molecules, because Si favors only sp^3 hybridization, which requires

   certain direction to get maximum overlap.

3) For linear structures, clusters with even total number of atoms have triplet

   ground state structures. Because in this situation, Si atom always at the

   end of the molecule, the C atoms next to Si atom has triple bonds, for Si

   atom has 4 electrons in its valence shell, one of them form a single bond

   with C atom, two of them form the lone pair of electrons and form a stable

   structure, therefore there is one single electron is left behind at one of the

end of linear molecule. Similarly there is another electron left behind at another end of this molecule, so there are two unpaired electrons in the molecules. They prefer triplet state as their lowest energy state.

4) Linear structure clusters with odd total number of atoms have singlet ground state structures. The bonding in these molecules is different from the case discussed in (3). However, one can use same principle to interpret it. Because of the symmetry, C-C atom bonds form double bonds, Si atoms still prefer go terminal position here have sp hybridization instead of sp_3 hybridization, and sharing two additional electrons to form the double bonds with C atom adjacent to Si, then the rest of the electrons of Si atom form a lone pairs electrons which proves to be a stable structure. Since both Si atoms at end of the molecules have paired electrons, the multiplicity is zero, so the clusters have singlet ground state structures.

5) Three ring bonding (one Si atom and two C atoms), four ring bonding (two Si atoms and two C atoms with Si atoms separate by C atoms) and six ring bonding (two Si atoms and four C atoms, Si atoms are separated by C atoms) have stable structures. The Si atoms still go to terminal positions, and C-C atoms are multi-bonded.

6) As the number of silicon atoms increase to 3 or more, there is no linear ground state structure found. The mixed silicon carbide clusters tend to show characteristics like pure silicon clusters having non-linear structures when silicon atoms increase to 3 or more in the Si_mC_n cluster

$m \times n = 4 \times 4$ system. In a same manner, when the numbers of carbon atoms are more than the number of silicon atoms, the cluster tends to show characteristics of pure carbon clusters, having linear structures.

7) Some of the structures of clusters changed for different electronic states (singlet, triplet, and doublet state). The triplet state has longer bond lengths and structures tend to expand. The doublet state structures are between the structures of singlet state and triplet state. All the structures that are bent and all silicon-rich clusters have singlet ground state. Triplet structures stretch out due to the differences in chemical bonding. For singlet state structure, the Si-C has double bonds or preferentially Si lone pairs. For triplet state structure, the Si-C has single bond. Double bond is stronger than single bond, and it is shorter than single bond. Therefore, the Si-C distance is larger in triplet state than in the singlet state.

5.2.2. Compare DFT Results with Experimental Results. Comparing the DFT EA results with experiment results, the largest absolute error is -0.178 eV (7%), the smallest absolute error is -0.042 eV (1.9%), and the average root mean square error is less than -0.1 eV, for the medium size of basis set level cc-pVDZ+ calculation. DFT gives same tendencies as experiment EA results; therefore one can conclude that DFT predicts very stable and accurate EA results.

5.2.3. Geometry Does Not Change Much with Different Basis Sets. Two

clusters are selected to investigate the geometry change using different size of

basis set. They are linear, carbon-rich cluster Si_2C_4 and bent, silicon-rich cluster

Si_3C. A represents the structure optimized using basis set cc-pVDZ, B represents

the structure optimized using basis set cc-pVTZ+. The numbers of basis

functions of cpVTZ+ are 3 times more than the number of basis functions of basis

set cc-pVDZ. The difference between A and B in bond length is about 0.011 Å,

in bond angle is 0.048°. One can conclude that the geometry change is very small

when increasing the basis set from cc-pVDZ to cc-pVTZ+. Similarly, the electron

affinity shows almost no difference between A and B. One can conclude that the

geometry and the electronic properties of clusters are not affected by their

optimizing basis set after the basis set reached a certain point. In SiC system, this

point is at basis set of cc-pVDZ.

5.2.4. Accuracy of Electron Affinity Calculation versus Basis Sets. The

size of basis set effects the accuracy of DFT energy calculations. Enlarging the

size of basis set without adding diffuse function improved the energy of singlet

state and triplet state energy by 4%. Only adding diffuse functions to basis set

improved the doublet state energy by 13%. So adding diffuse function to basis set

improved the electron affinity significantly. However, the electron affinity result

is determined by the difference between ground state energy (singlet or triplet)

and the doublet energy. By adding diffuse functions and increasing the basis set

size at same time, the calculation improvements are both to ground state energy

and doublet state energy. Subtraction of these two energies in the electron affinity calculation will cancel out large amount of accuracy improvements.

5.2.5. CPU Time Scale of DFT Calculations Conclusion.
The CPU time per SCF iteration increases with the number of basis functions with a scaling exponent on the order of 1.002. The powers of the exponential relation are different with choice of basis set. The scaling power increases with the size of basis set.

The total CPU time for each single point calculation is dependent on what the basis set. They have following order: cc-pVTZ+ > cc-pVDZ+ >cc-pVTZ. The total CPU time increases exponentially with adding carbon atoms to the SiC system to the order of 1.6^{th} power using cc-pVTZ+ basis set. The total CPU time increase exponentially with added silicon atoms to the SiC system on the order of the 2.2th power using cc-pVDZ+ basis set.

5.2.6. AM1 Calculation Method Summary.
AM1 predicts poor structures for SiC system, the bond length is too short, and the three-dimensional structures are not accurately predicted by the AM1 method.

AM1 method does not provide the reliable energy results for SiC system. Comparing the electron affinity results calculated by AM1 method with the experimental results, AM1 results oscillate badly relative to the experimental results while DFT predicts consistently accurate results. Two bad results of AM1 calculation come from cluster Si_3C and cluster Si_2C_4. For Si_3C, AM1 predict the

94

triplet ground state, DFT predicts the singlet ground state. Comparing the

electron affinity result, DFT gives more accurate results than AM1 method.

5.3 Possible Experimental Error

All the DFT calculation is in very good agreement with experiment results

in geometries, electron affinities and vibration frequencies, except cluster C_6Si_2.

Since the experimental result of vibration frequency is 3735 cm^{-1} for C_6Si_2, is

impossibly high, one suspicions that it might be an error in the experiment.

Therefore, all the comparison studies in this paper are not included comparison

with cluster C_6Si_2.

Appendix A: Calculation Method Abbreviation and Description

Semi-empirical calculation methods:

AM1   - using AM1 Hamiltonian [30, 35-36, 40-41]

CNDO   - using CNDO Hamiltonian [28]

INDO   - using INDO Hamiltonian [29]

MNDO   - using MNDO Hamiltonian [30, 32-39, 41]

PM3   - using MP3 Hamiltonian [42-43]

In semi-empirical calculations, different basis sets are not used; instead they use parameterized Hamiltonian from experiment results as substitution for integrals in quantum calculations.

Ab initio calculation:

HF-SCF – using Hartree-Fock average potential substitute the electron-electron interaction repulsive potential in Hamiltonian, and using self-consistence-field (SCF) iteration process to calculate the HF lowest energy.

CI   - configuration interaction (CI), is an improvement calculation base on HF but brought correlation energy by reprinting exact wave function as a linear combination of N-electron trial functions and use the linear variational method. If the basis were complete, the exact energies will be obtained not only of the ground state but also of all excited stats of the system.

QCISD - A quadratic CI calculation [59], including single and double substations. Also called CCSD

MP2 through MP5 – Based on a Hartree-Fock calculation (RHF for singlet, UHF for higher multiplicities) followed by a Moller-Plesset correlation energy

correction [47], and terminate at second-order called MP2 and terminated at fifth-order called MP5 [51].

MCSCF – The multi-configuration self-consistent field calculation, using a multi-determinant wave function, containing a relatively small number of configurations, which vary the orbitals to minimize the energy.

GVB -- The general valence bond (GVB) calculation, using the generalize balance bond wave function of W. A. Goddard III al et., can be treat as a special form of MCSCF wave function.

CAS – The completed active space calculation, which combine the SCF computation with a full CI involving with a subset of orbitals, which is known as the active space. This is a very high-level ab initio calculation.

Density Functional Method (DFT):

In Hartree-Fock theory, the energy has the form:

$$E_{HF} = V + <h\rho> + \frac{1}{2}<PJ(\rho)> - \frac{1}{2}<PK(\rho)>$$

Where V is the nuclear repulsion energy, P is the density matrix, $1/2<h\rho>$ is the classical coulomb repulsion of the electrons, and $-1/2<PK(\rho)>$ is the exchange energy resulting form the fermion's nature of electrons.

In DFT, the energy has the form:

$$E_{HF} = V + <h\rho> + \frac{1}{2}<PJ(\rho)> + E_x[\rho] + E_c[\rho]$$

Where $E_x[P]$ is the exchange functional, and $E_c[P]$ is the correlation functional The difference with HF method is that, in HF case, the $E_c[\rho]=0$ and

$E_x[\rho] = -\frac{1}{2}<PK(\rho)>$, besides the exchange functional and the correlation

functional, there are three hybrid methods which include a mixture of Hartree-Fock exchange with DFT exchange-correlation.

Becke's 3 LYP (B3LYP) – is Beck's 3 parameter functional [26], which has the form:

$$A^* E_x^{Slater} + (1 - A)^* E_x^{HF} + B^* \Delta E_x^{Becke} + E_c^{VWN} + C^* \Delta E_c^{non-local}$$

Where the non-local correlation is provided by the LYP expression. The constants A, B, and C are those determined by Becke by fitting to the G1 molecule set.

Basis set:

STO-3G – using 3 optimized primitive Gaussian function to represent 1s Slater function. It is the minimal basis functions.

4-31G – based on the STO-3G, using two more functions for each of the minimal basis functions to improve the accuracy.

6-31G – based on 4-31G, using 6 primitive Gaussian functions for inner 1s shell instead of 4.

6-31G* - base on 6-31G, add polarization function, such as d-type function to the first row atoms.

6-31G** - base on 6-31G*, adding p-type function to H.

cc-pVDZ – using correlation-consistent basis set by adding a set of primitive s and p functions to the hybrid (sp)set.

cc-pVDZ + – based on cc-pVDZ , the neutral sets were augmented with additional functions optimized for the atomic anions. It also denote as cc-pVDZ+, "+" means added diffuse functions, it also denoted as aug- cc-pVDZ.

cc-pVTZ -- based on cc-pVDZ, but using tripe-zeta instead of double-zeta.

cc-pVTZ+ – based on cc-pVTZ , the neutral sets were augmented with additional functions optimized for the atomic anions. It also denote as cc-pVTZ+, "+" means added diffuse functions, it also denoted as aug- cc-pVTZ.

cc-pVQZ -- based on cc-pVDZ, but using quadruple-zeta instead of double-zeta.

cc-pVQZ+ – based on cc-pVQZ , the neutral sets were augmented with additional functions optimized for the atomic anions. It also denote as cc-pVQZ+, "+" means added diffuse functions, it also denoted as aug- cc-pVQZ.

cc-pV5Z -- based on cc-pVDZ, but using five-zeta instead of double-zeta.

cc-Pv5Z+ – based on cc-pV5Z , the neutral sets were augmented with additional functions optimized for the atomic anions. It also denote as cc-pV5Z+, "+" means added diffuse functions, it also denoted as aug- cc-pV5Z.

Appendix B: The Detailed Energy Data of AM1 Calculations for Si_mC_n

(m+n=6) Clusters

#1 is the lowest energy structure, ie., the ground state structure
#7 is the highest energy structure among listed isomers

Number of Structure		#1	#2	#3	#4	#5	#6	#7
C_5Si_1 (a.u.)	S_0	-26.157769	-26.175566	-26.119430	-26.136743	-26.101254	-26.083174	-26.047980
	T_0	-26.235437	-26.187797	-26.173659	-26.143063	-26.140844	-26.100410	-26.044123
	$S_0 - T_0$	0.077668	0.012231	0.054229	0.00632	0.03959	0.017236	0.0038574

Number of Structure		#1	#2	#3	#4	#5	#6	#7
C_4Si_2 (a.u.)	S_0	-24.655134	-24.653588	-24.533757	-24.441279	-24.592901	-24.521114	-24.563563
	T_0	-24.700703	-24.694256	-24.600236	-24.595110	-24.569361	-24.587497	-24.582852
	$S_0 - T_0$	0.045569	0.040668	0.066479	0.153831	-0.02354	0.066383	0.019289

Number of Structure		#1	#2	#3	#4	#5	#6	#7
C_3Si_3 (a.u.)	S_0	-23.02755	-22.988167	-23.025578	-22.936722	-22.966227	-23.016521	-22.972109
	T_0	-23.098609	-23.05104	-23.044579	-23.027449	-23.025540	-23.012889	-22.995861
	$S_0 - T_0$	0.071059	0.062873	0.019001	0.090727	0.059313	-0.003632	0.023752

Number of Structure		#1	#2	#3	#4	#5	#6	#7
C_4Si_2 (a.u.)	S_0	-21.443801	-21.389268	-21.291940	-21.248666	-21.315360	-21.323062	-21.311838
	T_0	-21.450578	-21.435154	-21.431154	-21.391419	-21.373265	-21.368737	-21.358832
	$S_0 - T_0$	0.006777	0.045886	0.139214	0.142753	0.057905	0.045675	0.046994

Number of Structure		#1	#2	#3	#4	#5	#6	#7
C_1Si_5 (a.u.)	S_0	-19.627295	-19.656747	-19.700308	-19.628229	-19.640077	-19.661001	-19.647772
	T_0	-19.72652	-19.725780	-19.700649	-19.683327	-19.677714	-19.669153	-19.665222
	$S_0 - T_0$	0.099225	0.069033	0.000341	0.055098	0.037637	0.008152	0.01745

Appendix C: Energy and Electron Affinity Calculations of AM1 Method and

DFT Method for Si_nC_m (m+n=6) Clusters

The energy of Si_mC_n (m+n=6) clusters calculated by AM1 method

Name of Cluster		C_5Si_1	C_4Si_2	C_3Si_3	C_2Si_4	C_1Si_5
Energy (a.u.)	S_0	-26.157769	-24.665134	-23.02755	-21.443801	-19.627295
	T_0	-26.235437	-24.700703	-23.098609	-21.450578	-19.727652
	$S_0 - T_0$	0.077668	0.035569	0.071059	0.006777	0.100357
	D_0	-26.358403	-24.742554	-23.182718	-21.501504	-19.727127
Electron Affinity EA (eV)		3.334	1.135	2.280	1.381	-0.001
Experiment EA (eV)			2.556			
Absolute Error (eV)			1.421			

The energy of Si_mC_n (m+n=6) clusters calculated by DFT: B3LYP/cc-pVDZ method

Name of Cluster		C_5Si_1	C_4Si_2	C_3Si_3	C_2Si_4	C_1Si_5
Energy (a.u.)	S_0	-497.743447	-731.199176	-982.668917	-1234.127178	-1485.57010
	T_0	-497.758631	-731.239083	-982.651510	-1234.057851	-1485.52253
	$S_0 - T_0$	0.015184	0.013597	-0.017407	-0.0069327	-0.04757
	D_0	-497.863275	-731.319902	-982.746645	-1234.156321	-1485.58286
	EA (eV)	2.837	2.191	2.107	0.790	0.346
Experiment EA (eV)			2.556			
Absolute Error (eV)			0.365			

Appendix D: The Detailed Energies Calculated by DFT Method

Optimizing using DFT: B3LYP/cc-pVDZ

The Singlet energy of Si_mC_n Clusters

n	m=1	2	3	4
1	-327.348388	-617.012168	-906.533938	-1196.021594
2	-365.545578	-655.071615	-944.601121	-1234.127178
3	-403.396487	-693.180817	-982.636555	-1272.171562
4	-441.70654	-731.199176	-1020.728641	-1310.23311

The Triplet energy of Si_mC_n Cluster

n	m=1	2	3	4
1	-327.370509	-616.916731	-906.482154	-1195.930076
2	-365.469262	-654.986419	-944.575858	-1234.05817
3	-403.589924	-693.049315	-982.609495	-1272.153112
4	-441.638158	-731.239083		-1310.204553

The Doublet energy of Si_mC_n Cluster

n	m=1	2	3	4
1	-327.370509	-617.042556	-906.581475	-1196.101824
2	-365.593016	-655.115562	-944.649768	-1234.156321
3	-403.678161	-693.235051	-982.679133	-1272.233551
4	-441.780051	-731.319902	-1020.788808	-1310.308155

The Lowest energy of Si_nC_m Cluster (singlet or triplet)

m	n=1	2	3	4
1	-327.370509	-617.012166	-906.533938	-1196.021594
2	-365.545578	-655.071615	-944.601121	-1234.127178
3	-403.589924	-693.180817	-982.668917	-1272.171562
4	-441.70654	-731.239083	-1020.728641	-1310.23311

Adding a Si atom in anion cluster requiring energy

	Only one Si	add one Si	add one Si	add one Si
1	0	-289.641657	-289.521772	-289.487656
2	0	-289.526037	-289.529506	-289.526057
3	0	-289.590893	-289.4881	-289.502645
4	0	-289.532543	-289.489558	-289.504469

Adding a C atom in anion cluster requiring energy

m	1	2	3	4
n				
1 C	0	0	0	0
2 C	-38.2225065	-38.073006	-38.068293	-38.054497
3 C	-38.0851455	-38.119489	-38.029365	-38.07723
4 C	-38.10189	-38.084851	-38.109675	-38.074604
Ave	-38.136514	-38.09244867	-38.069111	-38.068777

The average energy required to add a Si atom vs. C atom ratio as:

Si:C

7.605263158

Single Point Calculation using DFT: B3LYP/cc-pVDZ+

The Singlet energy of Si_nC_m Cluster

	m 1	2	3	4	
n					
1		-617.016211	-906.537778	-1196.026056	-1485.574892
2	-365.611716	-655.075402	-944.605417	-1234.132368	
3		-693.185480	-982.674490	-1272.176143	
4	-441.712855	-731.245443	-1020.736236	-1310.239242	
5		-769.418134			
6					

The Triplet energy of Si_nC_m Cluster

	m 1	2	3	4
n	-327.393520			
1				
2	-365.470021			
3	-403.595652			
4		-731.245443		
5				
6		-807.411431		

The Doublet energy of Si_nC_m Cluster

	m 1	2	3	4	5
n					
1	-327.476826	-617.050531	-906.592754	-1196.111336	-1485.5760
2	-365.611716	-655.126418	-944.662163	-1234.167934	
3	-403.694959	-693.247601	-982.759190	-1272.245072	
4	-441.797125	-731.333142	-1020.805843	-1310.317387	
5	-479.879882	-769.425174			
6		-807.510607			

Appendix E: The Detailed Data of DFT Time Scaling

Name of Cluster	CPU time per SCF (sec.) cc-pVDZ+	CPU time per SCF (sec.) cc-pVTZ	CPU time per SCF (sec.) cc-pVTZ+
C_2Si_2	148.75		
C_3Si_2	223.57	68.7	380
C_4Si_2	326.09	90.15	616.56
C_5Si_2	720	320.34	1760
C_6Si_2	993	325.37	1858

Name of Cluster	CPU time per SCF (sec.) cc-pVDZ+ Average	CPU time per SCF (sec.) Singlet or Triplet	CPU time per SCF (sec.) Doublet
C_2Si1	38.22027972	38.07692308	38.36363636
C_2Si_2	148.75	144.5	153
C_2Si_3	542.98	527.71	558.25
C_2Si_4	1379.055	1410.36	1347.75
C_3Si1	124.725	101.7	147.75
C_3Si_2	264.715	234.29	295.14
C_3Si_3	725.375	700	750.75
C_3Si_4	1835.33	1808.44	1862.22

Reference

1. Amorphous and Crystalline Silicon Carbide", J.A. Powell , edited by G.L. Harris and W. Yang (Springer, Berlin, 1989), P.3.

2. H. N. Walternburg and J.T. Yates, Jr., Chem. Rev. 95, 1589 (1995)

3. A. D. Beck, J. Chem. Phys. 98, 5648 (1993)

4. J. R. Shoemaker, Ph.D dissertation, Air Force Institute of Technology (1997), P10-60

5. C. M. L. Rittby, American Institute of Physics, 175 1994

6. C. M. L. Rittby, J. Chem. Phys. 96 (9), 1992

7. C. M. L. Rittby, J. Chem. Phys. 95 (8), 1991

8. Z. H. Kafafi, R. H. Hauge, L. Fredin, and J. Margrave, J. Phys. Chem. 87, 797 (1983)

9. H. Kranze and W. R. M. Graham, J. Chem. Physs. 96, 2517 (1992)

10. P. A. withey and W. R. M. Graham, J. Chem. Phys. 96, 4068 (1992)

11. J. D. Prsilla-Marquez and W. R. M. Graham, J. Chem. Phys. 87, 5612, (1991)

12. V. D. Gordon, American Institute of Physics, 113 (13) 2000

13. M. C. McCarthy, A. J. Apponi, V.D. Gordon, J. Chem. Phys. 111, 6750 (1999)

14. X. Duan, L.W. Burggraf, D. Weeks, (going to be published, 2001)

15. Dr. Lineberger, Professor of University of Colorado, using photoelectron

spectroscopy technique recorded the electron affinity, vibration frequency modes, and ground state geometry of several clusters. They observed the linear cluster C_3Si, C_5Si_2, C_6Si_2 at room temperature and recorded the rhomboidal cluster CSi3 at the cooled temperature. They were not able to observe any other rich silicon clusters even at the cooled condition.

16.   Cheol Ho Choi and Mark S. Gordon (it is going to be published), September 11, 2000

17.   K. Raghavachari and J. S. Binkley, J. Chem. Phys. 87 (2191 (1987)

18.   J. M. L. Martin, J.P. Fransois, and R. Gijbels, J. Chem. Phys. 59, 8850 (1990)

19.   K. Raghavachari, J. Chem. Phys. 84m 5672 (1986)

20.   K. Raghavachari and C. M. Rohlfing, J. Chem. Phys. 89, 2219 (1988)

21.   Attila Szabo and Neil S. Ostlund, "Modern Quantum Chemistry", Dover publications, INC. 1996, P111-190

22.   M. J. S. Dwar, E. G. Zoebisch, E. F. Healy, and J. J. P. Stewart. AM1: A new general quantum mechanical molecular model. J. A,. Chem. Soc., 107: 3902, 1985.

23.   John A. Pople, David L. Beveridge, "Approximate Molecular Orbital Theory", McGraw-Hill Book Company, P45-130

24.   Robert G. Parr and Weitao Yang, "Density-Functional Theory of Atoms and Molecules", Oxford Science Publications, P3-35

25.   A. D. Becke, J. Chem. Phys. 98, 1372 (1993)

26.   A. D. Becke, "Density-functional thermochemistry. III. The role of exact

exchange" J. Chem. Phys. 98, 5648 (1993)

27.   R. Car and M. Parrinello. "Unified approach for molecular dynamics and density-functional theory". Phy. Rev. Lett., 55: 2471, 1985

REPORT DOCUMENTATION PAGE			Form Approved OMB No. 074-0188

The public reporting burden for this collection of information is estimated to average 1 hour per response, including the time for reviewing instructions, searching existing data sources, gathering and maintaining the data needed, and completing and reviewing the collection of information. Send comments regarding this burden estimate or any other aspect of the collection of information, including suggestions for reducing this burden to Department of Defense, Washington Headquarters Services, Directorate for Information Operations and Reports (0704-0188), 1215 Jefferson Davis Highway, Suite 1204, Arlington, VA 22202-4302. Respondents should be aware that notwithstanding any other provision of law, no person shall be subject to an penalty for failing to comply with a collection of information if it does not display a currently valid OMB control number.
PLEASE DO NOT RETURN YOUR FORM TO THE ABOVE ADDRESS.

1. REPORT DATE (DD-MM-YYYY) 01-03-2001	2. REPORT TYPE Master's Thesis	3. DATES COVERED (From – To) Sep 2000 –March 2001

4. TITLE AND SUBTITLE	5a. CONTRACT NUMBER
USE OF QUANTUM MECHANICAL CALCULATIONS TO INVESTIGATE SMALL SILICON CARBIDE CLUSTERST	5b. GRANT NUMBER
	5c. PROGRAM ELEMENT NUMBER

6. AUTHOR(S)	5d. PROJECT NUMBER
Jean W. Henry	5e. TASK NUMBER
	5f. WORK UNIT NUMBER

7. PERFORMING ORGANIZATION NAMES(S) AND ADDRESS(S)	8. PERFORMING ORGANIZATION REPORT NUMBER
Air Force Institute of Technology Graduate School of Engineering and Management (AFIT/EN) 2950 P Street, Building 640 WPAFB OH 45433-7765	AFIT/GAP/ENP/01M-4

9. SPONSORING/MONITORING AGENCY NAME(S) AND ADDRESS(ES)	10. SPONSOR/MONITOR'S ACRONYM(S)
Air Force Office of Scientific Research Attn: Mr. Michael R. Berman 801 North Randolph Street Room 732, Arlington VA 22203-1977 (703) 696-7781	11. SPONSOR/MONITOR'S REPORT NUMBER(S)

12. DISTRIBUTION/AVAILABILITY STATEMENT

APPROVED FOR PUBLIC RELEASE; DISTRIBUTION UNLIMITED.

13. SUPPLEMENTARY NOTES

14. ABSTRACT
   Density Functional Theory (DFT) method was employed to model silicon carbide small clusters. Comparing the DFT calculation results with experimental results that observed by using photoelectron spectroscopy (PES), DFT predicts the same structures that experiment observed. For electron affinity, DFT results are in good agreement with experimental results, the root mean square negative offset 0.1 eV found using medium size of basis set (cc-pVDZ+) calculation. DFT results for vibrational frequencies are in good agreement with experiment results; the root mean square error is 72.5 cm^{-1} wave number. 16 ground state structures of Si_mC_n ($m \leq 4, n \leq 4$) clusters were found using DFT:B3LYP/cc-pVDZ calculations, the properties of these structures were discussed. The calculation accuracy of electron affinity is affected by the properties of basis sets. Increasing basis set size improves the energy results of singlet and triplet state more than the energy result of doublet state; adding diffuse functions into basis sets dramatically improves the energy result of doublet state. Computational time scaling of DFT computations in SiC system was conducted. A brief an accuracy assessment study of AM1 semi-empirical method for Si_mC_n clusters was also performed.

15. SUBJECT TERMS
   Quantum Mechanics, Molecular Modeling, Computer Simulation, Surface Chemistry, Molecules, Atoms, Clusters
   Semi empirical, ab initio, Density Functional Theory (DFT)
   Schrödinger Wave Equation, Molecular Orbitals, Basis Sets, Basis Functions

16. SECURITY CLASSIFICATION OF:			17. LIMITATION OF ABSTRACT	18. NUMBER OF PAGES	19a. NAME OF RESPONSIBLE PERSON Prof. Larry W. Burggraf, ENP
a. REPORT	b. ABSTRACT	c. THIS PAGE			19b. TELEPHONE NUMBER (Include area code) (937) 255-3636, ext 4507
U	U	U	UU	119	

Standard Form 298 (Rev. 8-98)
Prescribed by ANSI Std. Z39-18

Form Approved OMB No. 074-0188